

Hedgehog signalling is required for correct anteroposterior patterning of the zebrafish otic vesicle

Katherine L. Hammond, Helen E. Loynes, Amos A. Folarin, Joanne Smith and Tanya T. Whitfield*

Centre for Developmental Genetics, University of Sheffield School of Medicine and Biomedical Science, Western Bank, Sheffield S10 2TN, UK

*Author for correspondence (e-mail: t.whitfield@sheffield.ac.uk)

Accepted 18 December 2002

SUMMARY

Currently, few factors have been identified that provide the inductive signals necessary to transform the simple otic placode into the complex asymmetric structure of the adult vertebrate inner ear. We provide evidence that Hedgehog signalling from ventral midline structures acts directly on the zebrafish otic vesicle to induce posterior otic identity. We demonstrate that two strong Hedgehog pathway mutants, *chameleon* (*con^{tf18b}*) and *slow muscle omitted* (*smu^{b641}*) exhibit a striking partial mirror image duplication of anterior otic structures, concomitant with a loss of posterior otic domains. These effects can be phenocopied by overexpression of *patched1* mRNA to reduce Hedgehog signalling. Ectopic activation of the

Hedgehog pathway, by injection of *sonic hedgehog* or dominant-negative *protein kinase A* RNA, has the reverse effect: ears lose anterior otic structures and show a mirror image duplication of posterior regions. By using double mutants and antisense morpholino analysis, we also show that both *Sonic hedgehog* and *Tiggy-winkle hedgehog* are involved in anteroposterior patterning of the zebrafish otic vesicle.

Key words: Hedgehog, Sonic hedgehog, Tiggy-winkle hedgehog, Inner ear, Zebrafish, Mirror image duplication, *slow muscle omitted*, *chameleon*, Otic vesicle, Axis formation

INTRODUCTION

The inner ears of vertebrates are responsible for the sensations of hearing and of balance. Although the two ears are symmetric about the midline of the organism, each individual organ in most vertebrate species is asymmetric about all three axes [anteroposterior/rostrocaudal (AP), dorsoventral (DV) and mediolateral (ML)]. The zebrafish otic field (defined by the expression of *pax8*) is induced at the lateral edges of the neural plate, adjacent to several presumptive rhombomeres (r) of the developing hindbrain. By about 14 hours post fertilisation (hpf), condensation of cells gives rise to distinct thickenings (the otic placodes) immediately opposite r5 (Kimmel et al., 1995; Pfeffer et al., 1998; Phillips et al., 2001). The expression of several genes, for example *pax2a* (formerly *pax2.1*), *dlx3b* (formerly *dlx3*) and *eya1*, is now detected throughout these placodes (Krauss et al., 1991; Akimenko et al., 1994; Sahly et al., 1999). The only known genes with restricted patterns of expression in the otic placode at this stage are the Delta genes. These are expressed in anterior and posterior domains, symmetrical about the AP and DV axes, but restricted to the medial side of the placode (Haddon et al., 1998). It is therefore likely that at 14 hpf only the ML axis of the otic placode has been specified.

Asymmetric gene expression patterns about both the AP and the DV axes are obvious by 18 hpf, when the placode begins

to cavitate to form an otic vesicle. *nkx5.1* (*hmx3* – Zebrafish Information Network), which is currently the earliest known marker of an asymmetry about the AP axis, is expressed in an anterior domain from around 16 hpf; *pax5* is detectable in the anterior epithelium from 17.5 hpf and *dacha* is detected in the dorsal otic epithelium by 17-18 hpf, suggesting that all axes of the ear have been specified by this time (Pfeffer et al., 1998; Adamska et al., 2000; Hammond et al., 2002). By 24 hpf, several further otic genes are expressed asymmetrically, and this presumably both reflects and reinforces axis specification. *pax5*, *nkx5.1* and *fgf8* are expressed anteriorly, *bmp7* and *follistatin* posteriorly, *dlx3b* and *dacha* dorsally, *eya1* ventrally, and *pax2a* and *dacha* medially (Krauss et al., 1991; Akimenko et al., 1994; Pfeffer et al., 1998; Reifers et al., 1998; Sahly et al., 1999; Adamska et al., 2000; Mowbray et al., 2001; Hammond et al., 2002). Sensory epithelium now thickens and stratifies, and fingers of non-sensory epithelium protrude into the otic lumen and fuse to form the semicircular canal system (reviewed by Whitfield et al., 2002).

Fekete and colleagues have proposed a model in which tissues surrounding the ear provide inductive signals for both axis specification and further otic differentiation (Fekete, 1996; Brigande et al., 2000a; Brigande et al., 2000b). They propose that signals from the hindbrain have dorsalising activity, and may also be important in providing AP information and medialising signals to the otic vesicle. Several lines of

evidence, ranging from early transplantation experiments carried out in *Amblystoma* to more recent studies of knockout and mutant mice, suggest that the hindbrain does provide signals to pattern medial and dorsal otic regions (Harrison, 1945; Deol, 1964; Mansour et al., 1993; Mark et al., 1993; McKay et al., 1996; Niederreither et al., 2000). Each hindbrain rhombomere also expresses a specific and unique group of genes, including members of the Hox gene cluster, and may thus impart AP identity to adjacent inner ear regions (Fekete, 1996; Prince et al., 1998; Brigande et al., 2000a; Brigande et al., 2000b).

Fekete and colleagues also suggest that ventral midline structures (i.e. the notochord and floorplate) may specify ventral otic structures. Both the notochord and floorplate are strong sources of Hedgehog (Hh) proteins, and evidence from the chick suggests that these tissues are able to repress dorsal and lateral otic fate (Giraldez, 1998). We therefore set out to test whether Hedgehog signalling from the ventral midline is required to pattern the developing ear, and in particular whether it is responsible for the specification and development of ventral and/or medial otic structures. Hh proteins are secreted peptides known to act as morphogens in the axis specification of other organs, such as the neural tube, limb bud and somites (Echelard et al., 1993; Krauss et al., 1993; Riddle et al., 1993; Roelink et al., 1995) (reviewed by Hammerschmidt et al., 1997; Ingham and McMahon, 2001). In many situations, Hh is a diffusible molecule, and, in vertebrates, has been reported to act over several cell diameters (up to 300 µm in chick limb bud mesenchyme, for example) (Gritli-Linde et al., 2001; Lewis et al., 2001; Zeng et al., 2001). Details of the signalling pathway have been elucidated in *Drosophila*. The Hh receptor, patched (Ptc), in the absence of Hh ligand, interacts with, and inhibits the action of, Smoothened (Smo). In the presence of Hh, repression of Smo via Ptc1 is lifted, and the signal is transduced through various intercellular intermediates to the transcription factor cubitus interruptus (Ci). Among the targets of the Hh signalling cascade is *ptc* itself, whose transcription is upregulated by active Hh signalling (for a review, see Ingham and McMahon, 2001).

In zebrafish, four hedgehog homologues have been reported: *sonic hedgehog* (*shh*) and *tiggy-winkle hedgehog* (*twhh*) (both orthologues of tetrapod *Shh*), and *echidna hedgehog* (*ehh*) and *hh-a* (orthologues of *Indian hedgehog*) (Krauss et al., 1993; Ekker et al., 1995; Currie and Ingham, 1996; Zardoya et al., 1996a; Zardoya et al., 1996b). Components of the transduction cascade include two Patched genes, and at least three Gli genes, orthologues of *ci* (Concordet et al., 1996; Karlstrom et al., 1999; Lewis et al., 1999a; Varga et al., 2001). Importantly, only a single *smoothened* orthologue, *smo*, appears to have been retained in the zebrafish genome, and all Hh signalling is thought to require the function of this gene (Varga et al., 2001). Mutations in some components of the Hh pathway have been isolated: *shh* is disrupted in *sonic you* (*syu*) mutants, *gli1* is disrupted in *detour* (*dtr*) mutants, *gli2* is disrupted in *you too* (*yot*) mutants and the *smo* gene is disrupted in mutant alleles of *slow muscle omitted* (*smu*) (Schauerte et al., 1998; Karlstrom et al., 1999; Barresi et al., 2000; Chen et al., 2001; Varga et al., 2001; Karlstrom et al., 2003). In addition, the Hh pathway is thought to be disrupted in *chameleon* (*con*), *iguana* (*igu*) and *you* mutants (Schauerte et al., 1998; Lewis et al., 1999b; Odenthal et al., 2000).

Consistent with a role for Hedgehog in early medial or ventral otic patterning, we find that all essential components of the Hh signal transduction cascade are expressed in the otic vesicle, while three *hh* genes are expressed in adjacent midline structures (notochord and floorplate). Surprisingly, however, mutant analysis indicates that Hh signalling appears to be involved in AP patterning of the otic vesicle, rather than DV or ML patterning as predicted. Using double mutants and antisense morpholino experiments, we also show that both *Shh* and *Twhh* are involved in this AP patterning, and that either gene alone can compensate for the absence of the other.

MATERIALS AND METHODS

Zebrafish stocks

Wild-type embryos used were WIK or AB. Mutant strains used were *conf18b*, *cycf219*, *dtr^{ts269}*, *flhk241* or *flh^{im229}*, *igu^{ts294}*, *ntl^{tc41}*, *oep^{t2257}*, *smu^{b641}*, *syu^{t4}* and *yot^{ty119}*, all recessive loss-of-function alleles, and *yot^{ty119}*, a dominant repressor of Gli-mediated Hh signalling. Phenotypically wild-type siblings were used as controls. Embryonic stages are given as hours post fertilisation (hpf) at 28.5°C, converted from somite stages in embryos younger than 24 hpf (Westerfield, 1995; Kimmel et al., 1995).

In situ hybridisation

Whole-mount in situ hybridisation was carried out as described previously (Oxtoby and Jowett, 1993). Digoxigenin-labelled probes were prepared according to manufacturer's instructions (Roche). For microscopy, embryos were cleared in a glycerol/PBS series and mounted in 100% glycerol. Sense hybridisations were carried out for *smo*, *gli2* and *ptc2*; all were negative.

FITC-phalloidin stain

Embryos were whole-mount stained for actin with FITC-phalloidin as described previously (Haddon and Lewis, 1996), mounted in Vectashield (Vector Laboratories) and imaged with a Leica SP confocal microscope. For dorsal views, ears were dissected.

Sections

After in situ hybridisation, embryos were fixed overnight in 4% paraformaldehyde, and cleared through a glycerol/PBS series. Sections (~100 µm) were cut using a hypodermic needle and mounted in 100% glycerol. For thinner sections, fixed embryos were embedded in 1% low melting point agarose to facilitate correct orientation. Agarose blocks were dehydrated and cleared in an ethanol/butanol series, embedded in paraffin wax, and sectioned at 7 µm. Sections were stained with Haematoxylin and Eosin, and mounted in DePeX (Sigma).

mRNA injection

5'-methylguanosine-capped sense mRNA was produced as described previously (Krieg and Melton, 1984). RNA (5 nl) was injected into one- or two-cell embryos using a Narishige microinjection rig, at 50 ng/µl to 1 µg/µl for *ptc1* RNA, 25 ng/µl to 100 ng/µl for *shh* RNA, 25 ng/µl to 400 ng/µl for dnPKA RNA (Concordet et al., 1996), and 500 ng/µl for *ehh* and *twhh* RNA. nGFP RNA (75 ng/µl) was co-injected in all experiments. GFP was visualised between shield stage and tail bud stage; embryos not expressing GFP ubiquitously were discarded.

Morpholino injection

Carboxyfluorescein-conjugated antisense morpholinos (GeneTools) were targeted to the 5' end of the *shh* and *twhh* open reading frames (GenBank Accession Numbers, AF124382 and U30710,

respectively). The sequences were: *shh* MO (5' to 3'), aag ccg cat ttt gcc gca cgc tga a; and *twhh* MO, gct tca gat gca gcc tta cgt cca t (Lewis and Eisen, 2001). Morpholinos (MOs) were diluted to 0.5 mM or 0.25 mM using Danieau medium (Nasevicius and Ekker, 2000) and injected into one- or two-cell embryos; any embryo not showing ubiquitous fluorescence was discarded. *twhh* MO (0.5 mM) caused necrosis at the anterior end of the embryo, which appears to be a nonspecific effect (data not shown).

Microscopy

For observation, embryos were anaesthetised with tricaine (3-amino benzoic acid ethyl ester) and mounted in 3% methyl cellulose (Westerfield, 1995). Initial analysis was carried out using a Leica MZ12.5 fluorescence dissecting microscope. Detailed examination and photography was carried out using an Olympus BX51 compound microscope, Olympus Camedia (C-3030ZOOM) camera and AnalySIS software (Olympus). Images were assembled using Adobe Photoshop.

RESULTS

Hh pathway genes are expressed in and around the developing ear

As a first step towards identifying possible roles for Hh signalling in otic vesicle development, we analysed mRNA expression patterns of zebrafish Hh pathway components in the vicinity of the ear (Fig. 1). None of the three zebrafish *hedgehog* genes examined, *twhh*, *shh* and *ehh*, are expressed in the otic vesicle itself. The closest source of Hedgehog to the ear between 16.5 hours post fertilisation (hpf) and 30 hpf is from midline tissues; *shh* is expressed in both the notochord and floorplate, while *twhh* is expressed only in the floorplate, and *ehh* only in the notochord (Fig. 1C,E,G) (Krauss et al., 1993; Ekker et al., 1995; Currie and Ingham, 1996). These structures are approximately 40 μ m from the vesicle at 24 hpf, which is a feasible distance over which Hh may act (Gritli-Linde et al., 2001; Lewis et al., 2001; Zeng et al., 2001). *shh* is also expressed in visceral endoderm from 24 hpf (Roy et al., 2001), and in pharyngeal endoderm from 30 hpf (Piotrowski et al., 2000). At 25 hpf, endodermal expression is about 75 μ m posterior to the ear, and is weaker than the floorplate expression nearer the ear (data not shown) (Roy et al., 2001). *twhh* expression is also detectable in the pharyngeal endoderm at 24 hpf, ~100 μ m from the otic vesicle (data not shown).

Genes encoding components for the reception and transduction of the Hh signal are expressed in the otic epithelium. *ptc1* is expressed in a ventromedial domain from 16.5 to 30 hpf, initially uniformly along the AP axis of the vesicle, but becoming concentrated in the posterior by 22 hpf (Fig. 1B,I,J). This indicates active Hh signal transduction in the otic vesicle, since *ptc1* is itself a transcriptional target of the Hh pathway (Concordet et al., 1996; Goodrich et al., 1996). *ptc2* is expressed similarly to but more widely than *ptc1*, as its expression is upregulated by a lower concentration of Hh signal (Lewis et al., 1999a). By 24 hpf, *ptc2* RNA is detectable throughout ventral otic epithelium of wild-type embryos, rather than being restricted to a *ptc1*-like ventromedial band (Fig. 1D). *smo* is expressed throughout the otic vesicle from 16.5 to 30 hpf (Fig. 1F). Thus, all reported essential components of the zebrafish Hh signalling pathway are expressed in locations

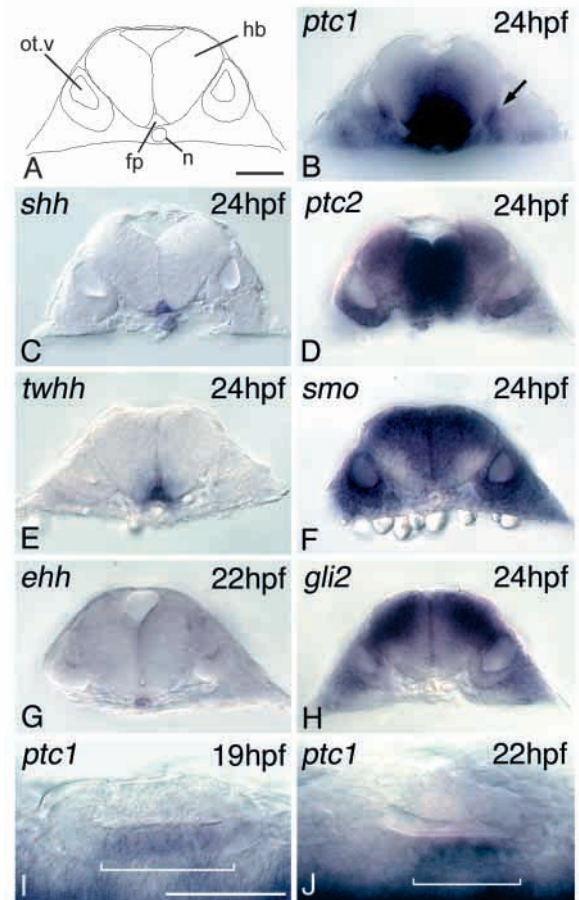


Fig. 1. Expression of Hedgehog pathway components in the zebrafish otic vesicle. (A) Tracing of transverse section, outlining relevant tissues: ot.v, otic vesicle; fp, floorplate; n, notochord; hb, hindbrain. Dorsal towards the top. Scale bar: 50 μ m. (B-H) Transverse, hand cut sections of whole-mount in situ hybridisation. Note that midline sources of Hedgehog are approximately 40 μ m from the otic vesicle; *shh* is expressed in both the floorplate and notochord (C), *twhh* in just the floorplate (E) and *ehh* in just the notochord (G). Factors necessary for transduction of the Hh signal are expressed within the otic vesicle; *ptc1* is expressed in a ventromedial domain (arrow, B), *ptc2* throughout ventral otic regions (D) and *smo* throughout the entire vesicle (F). *gli2* is not, however, highly expressed in the developing ear (H). (I,J) Dorsal views of whole-mount otic vesicle preparations. Anterior towards the left, lateral towards the top. Scale bar: 50 μ m. At 19 hpf (I), *ptc1* is expressed throughout the ventromedial otic vesicle but by 22 hpf (J) is concentrated in posterior regions (brackets).

consistent with a direct role for Hh in early ear development. *gli2*, however, is not highly expressed in the otic epithelium (Fig. 1H). It is possible, however, that another Gli gene is expressed here, as Gli genes are expressed differentially in other developmental contexts (reviewed by Ingham and McMahon, 2001).

Providing further evidence for a direct effect of Hh signalling on otic vesicle development, otic *ptc1* expression is greatly reduced or lost in two strong Hh pathway mutants, *conf18b* and *smu^{b641}* (Fig. 2A-C). In addition, *ptc1* expression is upregulated in the ears of embryos in which *shh* RNA has been overexpressed (Fig. 2D). In all three of these cases, an

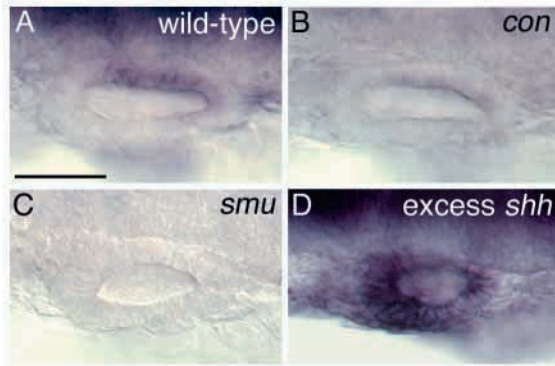


Fig. 2. Expression of *ptc1* in two Hh pathway mutants and in embryos in which *shh* RNA has been overexpressed. Dorsal views of 24 hpf whole-mount otic vesicle preparations showing *ptc1* expression. Anterior towards the left, lateral towards the bottom. Scale bar: 50 μ m. Note that *ptc1* expression is much weaker in *con^{tf18b}* homozygotes (B) than in wild-type embryos (A; a sibling of the *con^{tf18b}* homozygote). *ptc1* expression is undetectable in the *smu^{b641}* otic vesicle (C) and is upregulated throughout the vesicle in embryos in which *shh* has been overexpressed by injection of 100ng/ μ l *shh* RNA (D).

otic phenotype is associated with the alteration in *ptc1* expression, as discussed below.

The ears of *con^{tf18b}* and *smu^{b641}* homozygotes have AP patterning defects

To investigate the effect of reduced Hedgehog signalling on otic development, we analysed the ears of all zebrafish mutants known or presumed to be defective in a component of the Hh signalling pathway (Table 1). Only three of these show gross otic patterning defects. First, *con* and *smu* ears, contrary to expectation, display AP patterning defects, as described below. Second, the ears of *igu* mutants lack the dorsolateral septum that divides the anterior and posterior semicircular canals, but appear normal in all other respects (data not shown); this phenotype will not be considered further in this report.

By 72 hpf, the wild-type ear is well differentiated and displays clear asymmetries about all three axes (AP, DV and ML). The most obvious structures are the otoliths, which lie over the two maculae. The smaller, anterior (utricle) otolith

Table 1. Summary of ear phenotypes of the zebrafish Hh pathway mutants

Mutant strain	Gene mutated	Ear defect
<i>smu^{b641}</i>	<i>smo</i>	Anteriorised*
<i>con^{tf18b}</i>	Unknown	Anteriorised*
<i>syu^{t4}</i>	<i>shh</i>	Retarded but otherwise normal* [†]
<i>yof^{y119}</i>	<i>gli2</i>	None*
<i>dty^{m276}</i>	<i>gli1</i>	None*
<i>yout^{y97}</i>	Unknown	None*
<i>igu^{s294}</i>	Unknown	Dorsal septum absent* [‡]

*Supernumerary, untethered otoliths are often observed in all Hedgehog pathway mutants examined. Investigation (not detailed in this report) revealed that this is probably an artefact of the lack of spontaneous movement in the developing embryo and is not specific to Hh pathway mutants.

[†]The entire *syu^{t4}* embryo is developmentally retarded. Retardation of ear development is in line with that of the rest of the embryo.

[‡]Phenotype not described further in this report.

is situated ventral and lateral to the larger, posterior (saccular) otolith, which lies medially. In both *smu* and *con* the two otoliths are small, ventral and lateral, resembling the anterior otolith (Fig. 3A-C). The underlying maculae can be visualised by phalloidin staining, which labels the actin-rich stereociliary bundles of hair cells. In the ears of wild-type embryos, the anterior (utricle) macula sits on the anteroventral floor, and the posterior (saccular) macula lies on the posteromedial wall (Fig. 3D,G). In *smu*, however, a single sensory patch covers the entire ventral floor of the vesicle, while in *con* the anterior macula is present but an additional ventral sensory patch develops at the posterior of the ear (Fig. 3E,F,H,I). This second patch resembles a posterior macula in shape, but is reduced in size. In neither *smu* nor *con* is there a sensory patch in the normal medial position of the posterior macula (Fig. 3E,F). Note, however, that the position of the axes of the ear with respect to the midline is altered in *con* and *smu* homozygotes (Fig. 3J-L). Midline tissue is missing, bringing the ventral surface of the ear closer to the midline than normal. Taken together, these data suggest that posterior otic regions are not specified correctly in *smu* and *con*, and may be acquiring some anterior identity.

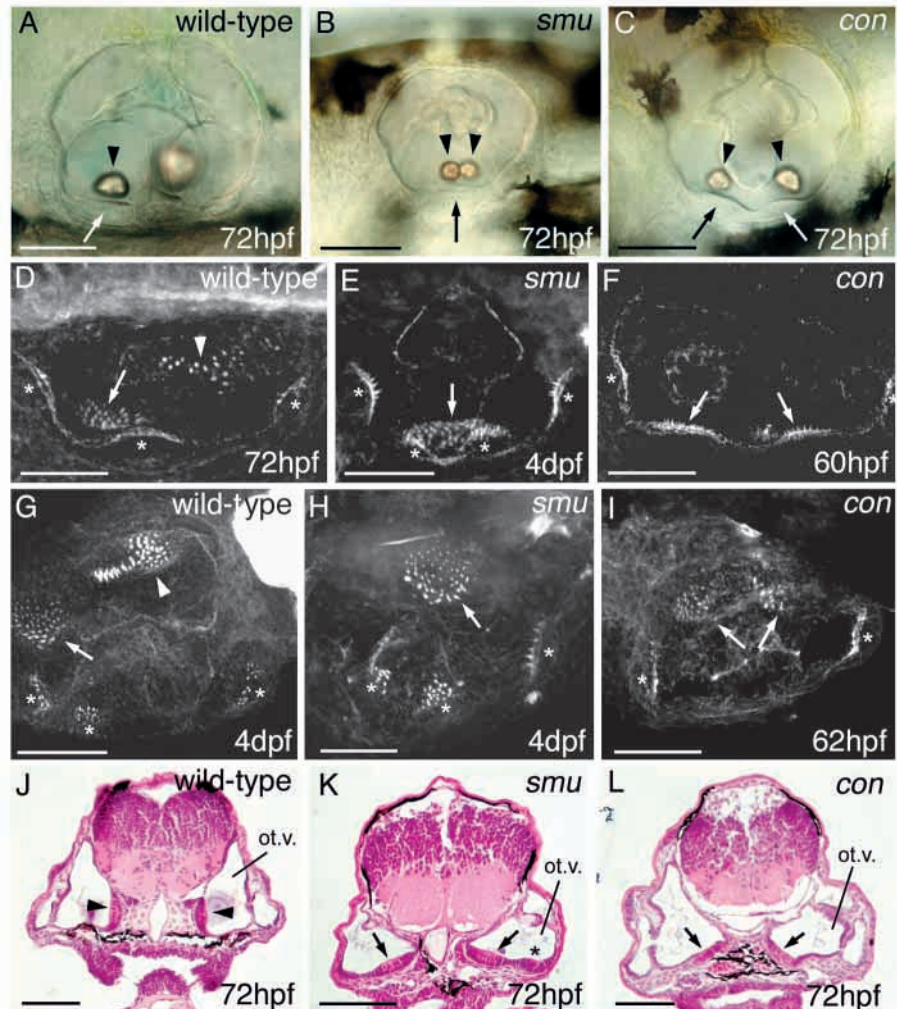
Posterior otic structures are lost in *smu^{b641}* and *con^{tf18b}* while anterior regions are duplicated

To investigate *smu* and *con* ear patterning in detail, we used a panel of otic region-specific markers. Anterior expression domains of three genes are duplicated or expanded into posterior regions of the otic vesicle of *smu* and *con* homozygotes. Anterior domains of *otx1* expression at 48 hpf are duplicated in a mirror image manner in both *con* and *smu* (Fig. 4A-C). Similarly, *wnt4* expression at 36 hpf, normally detectable at the posterior end of the anterior macula, shows duplicated expression at the anterior end of the second ventral macula in *con* (Fig. 4D,F). *wnt4* is also expressed in the centre of the single ventral macula in *smu* (Fig. 4E). Third, *nkx5.1*, which normally marks anterior otic regions from 16 hpf, and a small posterodorsal region by 30 hpf, is expanded along the entire AP extent of the ear in both *con* and *smu* (Fig. 4G-I). These expression domains suggest a duplication of anterior otic regions. However, *pax5* and *fgf8*, both of which mark anterior otic epithelium at 24 hpf, maintain their normal expression pattern in *con* and *smu*, suggesting that this duplication is incomplete (Fig. 4J-O). Confirming the absence of posterior identity, *folistatin* expression, which normally marks a localised posterior epithelial region from 24 hpf, is absent or severely reduced in the ears of both *con* and *smu* (Fig. 4P-R). Taking these data together, we conclude that a partial mirror image duplication of anterior otic regions occurs at the expense of posterior identity in *con* and *smu* homozygotes.

Dorsoventral and mediolateral patterning appear relatively normal in *con^{tf18b}* and *smu^{b641}* ears

Expression patterns of *dlx3b*, a dorsal otic marker, and *eyal*, a ventral marker, are normal in *con* and *smu* homozygotes (Fig. 4S-X). In addition, several of the genes discussed above with respect to AP patterning are expressed asymmetrically about the DV axis: *otx1*, *wnt4* and *nkx5.1* are all ventral markers (Fig. 4A-I). In all cases, it is only the AP patterning that is altered; the DV aspect of these expression patterns remains unaffected. In addition, a ventral neurogenic region is specified in *con* and

Fig. 3. The ears of *con^{tf18b}* and *smu^{b641}* homozygotes display a loss of posterior structures and a duplication of anterior structures. (A-C) DIC images of live ears, focussed at the level of the anterior otolith. Lateral views; anterior towards the left, dorsal towards the top. Both otoliths in *con* and *smu* ears (arrowheads, B,C) are small, lateral and ventral, resembling the anterior otolith (arrowhead, A) of wild-type embryos rather than the larger, medial posterior otolith (out of focus in A). Arrows indicate ventral sensory thickenings (maculae) underlying the otoliths. In the wild type, the anterior (utricle) macula lies under the anterior otolith on the ventral floor of the vesicle (A). In *smu*, a single ventral macula underlies the two small otoliths (B), while in *con*, a second ventral macula is found at the posterior of the ear (C). (D-I) Confocal images (projections of z-series) of ears stained with FITC-phalloidin to reveal the actin-rich stereocilia of sensory hair cells. (D-F) Lateral views; anterior towards the left, dorsal to top. (G-I) Dorsal views; anterior towards the left, medial towards the top. (D,G) Wild-type pattern. This is similar between 60 hpf and 4 dpf, but the number of hair cells increases in all patches during this time. Note the rounded anterior macula on the ventral floor of the vesicle (arrow) and the irregularly shaped posterior macula on the medial wall (arrowhead). Asterisks indicate the three cristae. In *con* and *smu*, the posterior macula is absent from the medial wall. In *smu*, a single ventral macula covers the ventral surface of the ear (arrow, E,H). In *con*, the anterior macula is present as normal (left arrow, F,I), but a second ventral macula is present at the posterior of the ear (right arrow, F,I). This resembles the posterior macula in shape but is smaller than normal. In a proportion of *con* and *smu* ears four cristae are present (E). (F,I) *con* ears with only two cristae, because of the relative immaturity of these ears. (J-L) Transverse paraffin sections (10 μ m) through the otic vesicles, stained with Haematoxylin and Eosin. Dorsal towards the top. ot.v, otic vesicle; arrows, ventral maculae; arrowheads, posterior (medial) maculae; asterisks indicate cristae. Midline tissue is lost between the otic vesicles of *smu* and *con* embryos, so that the vesicles turn inwards towards the midline. However, all sensory patches are ventral; none are found on the medial wall. Scale bars: 50 μ m.



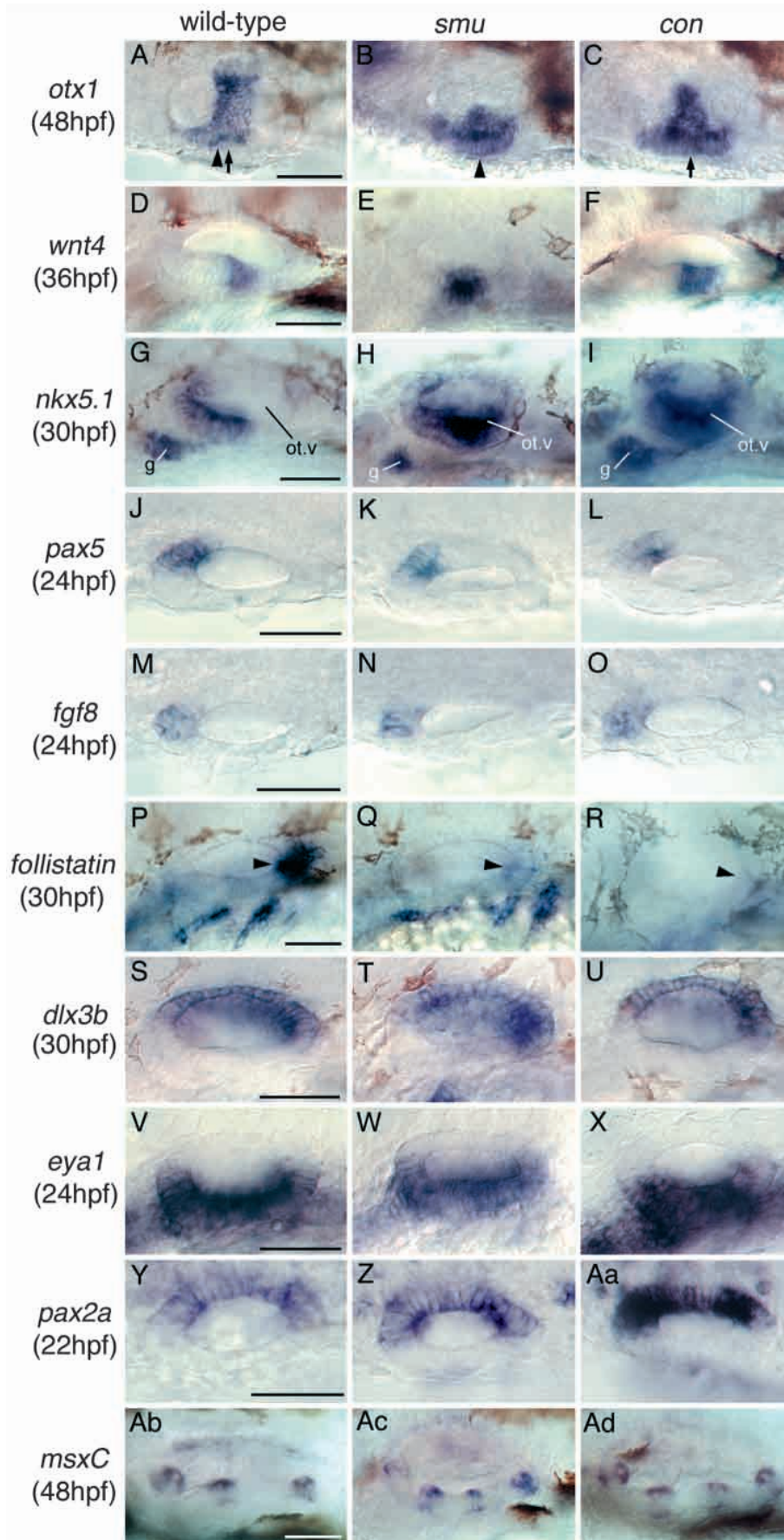
smu ears (see below). We therefore conclude that the DV otic axis is patterned correctly in the absence of Hh signalling. We are unable to tell, however, whether the dorsal part of the ear is also duplicated about the AP axis in *con* and *smu*, as semicircular canal projections appear symmetrical in the wild-type ear, and no AP-restricted dorsal markers are currently available. It is possible, therefore, that Hh is involved only in patterning ventral otic structures, and that other signals pattern the AP axis of dorsal regions.

The expression of *pax2a*, which marks the medial side of the otic vesicle, is also unchanged in *con* and *smu* homozygotes (Fig. 4Y-Aa). Likewise, the medial position of the *pax5* expression domain is normal (Fig. 4J-L). These data suggest that the ML axis of *smu* and *con* ears is also patterned correctly. We do observe a change in the medial expression of *otx1* (Fig. 4A-C). However, the medial expression of *otx1* normally marks the posterior macula (Fig. 4A); because this structure is missing in *smu* and *con*, we conclude that this change in *otx1* expression is a result of the anterior duplication, rather than a

separate ML patterning defect. Note also that ectopic cristae may develop in *smu* and *con* ears, while cristae are reduced or absent in the ears of embryos in which Hh signalling is increased (see below). These data suggest that Hh may repress the development of cristae, which are lateral structures, but in the mutants, ectopic cristae may be explained by the duplication of anterior regions.

A single statoacoustic ganglion is associated with each ear in *con^{tf18b}* and *smu^{b641}*

Neuroblasts that form the statoacoustic ganglion (SAG) delaminate from an anteroventral region of the otic epithelium and migrate anteriorly to form the ganglion, which is positioned anteroventral to the otic vesicle (Haddon and Lewis, 1996). As anterior regions of the otic vesicle are partially duplicated in the absence of Hh signalling, it was of interest to know whether signals from the vesicle might specify the direction of neuroblast migration. If so, we would predict that in *con* and *smu* mutants, neuroblasts would migrate both



anteriorly and posteriorly, forming a second ganglion underneath posterior regions of the ear. The presumptive SAG is thought to be marked by the expression of both *nkx5.1* and *sna2* expression at 24 hpf (Thisse et al., 1995; Adamska et al., 2000). In *con* and *smu* homozygotes, the expression of *nkx5.1* and *sna2* remains detectable in the SAG in an anterior domain of variable size, but there is no evidence of a posterior duplicated region of expression of either of these genes (Fig. 4G-I and data not shown). We conclude that the specification of neuroblasts in ventral regions does occur in *con* and *smu*, but that the direction of neuroblast migration is controlled independently of AP otic vesicle patterning.

Four cristae develop in a proportion of *con*^{tf18b} and *smu*^{b641} ears

At 48 hpf, both *bmp4* and *msxc* are expressed in three discrete ventral domains, representing the developing cristae (Ekker et al., 1997; Mowbray et al., 2001). A fourth expression domain of both of these genes is seen in 31% (5/16) *con* and 50% (5/10) *smu* ears, suggesting the presence of an ectopic crista (Fig. 4Ab-Ad and data not shown). Hair cells differentiate in these ectopic cristae (Fig. 3E). This phenotype is consistent with an anterior

Fig. 4. Gene expression in *con*^{tf18b} and *smu*^{b641} ears. Whole-mount in situ hybridisation; anterior towards the left. (A-C, J-O, Y-Aa) Dorsal views, medial towards the top. All other panels are lateral views, dorsal towards the top. Anterior otic expression domains of *otx1* (A-C), *wnt4* (D-F) and *nkx5.1* (G-I), but not *pax5* (J-L) and *fgf8* (M-O), are duplicated at the posterior of *smu* and *con* otic vesicles. Arrowhead (A,B) shows axis of *otx1* symmetry in *smu* ears. Arrow (A,C) shows axis of *otx1* symmetry in *con* ears. *nkx5.1* expression in the statoacoustic ganglion (g) is not duplicated at the posterior of the ear (G-I). Posterior expression domains of *follistatin* (arrowhead, P-R) are lost. Expression of dorsal (*dlx3b*, S-U), ventral (*eya1*, V-X) and medial (*pax2a*, Y-Aa) markers are not affected in *con* and *smu*. An ectopic expression domain of the crista marker *msxc* is present at the posterior of ~31% *con* and 50% *smu* mutants (Ab-Ad). ot.v, otic vesicle; g, statoacoustic ganglion. Scale bars: 50 μ m (shown in the left-hand panel of each set).

otic duplication in *con* and *smu*, as both the anterior and lateral cristae are located in the anterior half of the normal ear. An anterior duplication would, therefore, also lead to the presence of two cristae at the posterior of the ear. Owing to the lack of markers specific to individual cristae, however, we were unable to assign an identity to the cristae in the ears of *con* and *smu*.

ptc1 injection phenocopies the defects in *con*^{tf18b} and *smu*^{b641} mutant ears

To confirm that the ear phenotypes observed in *con* and *smu* are indeed caused by decreased Hh signalling, we overexpressed *ptc1* RNA in wild-type embryos. This mimics a loss of function Hh pathway mutant, as an excess of Ptc1 will exert a repressive effect on Smo (Goodrich et al., 1999). We injected 5 nl of *ptc1* RNA into one- or two-cell embryos at concentrations ranging from 0.05 µg/µl to 1 µg/µl. Concentrations below 0.5 µg/µl had no effect on the ear. However, at 0.5 µg/µl we phenocopied the *con* ear defects in approximately 21% of the ears examined. The remaining ears either had no defect or were too necrotic to classify (Fig. 5; Fig. 6E; Table 2). At 1 µg/µl, many embryos died due to nonspecific toxic effects; however, 1.5% ears now showed a slightly more severe phenotype resembling *smu* ears (Fig. 5; Fig. 6I; Table 2). This suggests that the *smu* ear phenotype is caused by a more severe reduction in Hh signalling than the *con* phenotype, and corroborates other studies that indicate that Hh signalling is more strongly attenuated in *smu* than *con* (Lewis et al., 1999b; Barresi et al., 2000; Chen et al., 2001; Varga et al., 2001).

Phalloidin staining of the ears from embryos injected with 0.5 µg/µl *ptc1* RNA confirmed the similarity of the phenotype to that seen in *con* (Fig. 6F): these ears lack a posterior macula, have a second ventral patch of hair cells at the posterior, and in a number of cases possess four cristae. Expression of *msxc* confirmed the presence of four cristae in 3/20 *con*-like ears examined (Fig. 6G). In addition, *nkx5.1* expression is expanded along the entire ventral aspect of the otic vesicle, confirming that the phenotype is identical to that seen in the loss of function Hh pathway mutants (Fig. 6H).

To confirm that the difference between the *con* and *smu* ear phenotypes is due to differences in the level of residual Hh activity, we injected 0.5 µg/µl *ptc1* RNA into embryos from a *con*/+ × *con*/+ mating. This should reduce Hh signalling further in the *con* homozygotes, but circumvents the use of toxic levels of *ptc1* mRNA. In 14.8% of ears from injected embryos, we observe a *smu*-like otic phenotype; these embryos presumably represent the homozygous *con* mutants. A further 16.1% of ears show a *con*-like phenotype; these embryos may include homozygous, heterozygous or wild-type siblings (Fig. 5; Table 2). The level of death due to nonspecific toxic effects of RNA

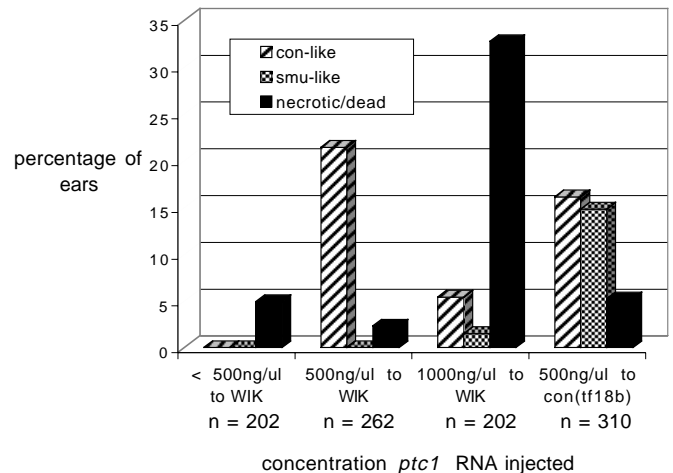


Fig. 5. Ear phenotypes caused by injection of *ptc1* RNA into one- or two-cell zebrafish embryos. *ptc1* RNA (5 nl), at the concentrations shown, was injected into one- or two-cell wild-type (WIK) embryos or embryos from a cross between two *con*^{tf18b} heterozygotes. Embryos were scored as wild type, *con* like or *smu* like or dead/necrotic based on their ear phenotype at 72 hpf (data are shown in Table 2). Most embryos were scored based on their appearance under a compound light microscope; confocal imaging of sensory hair cells was sometimes used for confirmation. The percentage of each phenotypic class is shown; all remaining embryos were wild type. Data from several batches of injections have been pooled. At 1000 ng/µl, *ptc1* RNA proved to be toxic, but at 500 ng/µl, injection into WIK resulted in 21% embryos developing with *con*-like ears, while injection into embryos from a *con*/+ mating results in 14.8% (the presumed *con* homozygotes) developing a *smu*-like ear phenotype.

injection is low (5.2%) and comparable with that seen in the wild-type injection experiments (Table 2). Phalloidin staining confirmed the similarity of the phenotype to that seen in *smu* ears: the posterior macula was absent, a single ventral macula was observed and four cristae were seen in some ears (Fig. 6J). No in situ markers were used, as we have found none that distinguishes between the *con* and *smu* ear phenotypes. The *ptc1* injection data therefore confirm that the difference between the *con* and *smu* ear phenotypes is due to a difference in Hh activity levels in the two mutants.

Both Shh and Twhh contribute to otic anteroposterior patterning

At least three Hedgehog genes are expressed in the vicinity of the ear (Fig. 1) but a mutant is available in only one of these, *syu*, which removes the function of Shh. There are as yet no reported zebrafish *twhh* or *ehh* mutants. To investigate which

Table 2. Ear phenotypes caused by *ptc1* RNA injection into one- or two-cell zebrafish embryos

Strain injected	Concentration of RNA (ng)	No AP defect	<i>con</i> like	<i>smu</i> like	Number necrotic or dead	Total
WIK (wild type)	50	28 (100%)	0	0	0	28
WIK	100	90 (93.8%)	0	0	6 (6.2%)	96
WIK	200	74 (94.9%)	0	0	4 (5.1%)	78
WIK	500	132 (78.5%)	30 (17.9%)	0	6 (3.6%)	168
WIK	500	68 (72.3%)	26 (27.7%)	0	0	94
WIK	1000	122 (60.4%)	11 (5.4%)	3 (1.5%)	66 (32.7%)	202
<i>con</i> ^{tf18b/+} × <i>con</i> ^{tf18b/+}	500	198 (63.9%)	50 (16.1%)	46 (14.8%)	16 (5.2%)	310

of these three zebrafish Hedgehog genes have a role in AP otic patterning, we therefore made use of the midline mutants *no tail (ntl)* and *cyclops (cyc)* in addition to *syu*. *ntl* mutants carry a mutation in the zebrafish homologue of the *Brachyury* gene and lack a differentiated notochord (Schulte-Merker et al., 1994). *ntl* embryos therefore never express *ehh* because *ehh* is expressed only in the notochord (Currie and Ingham, 1996). *cyc*, a *nodal*-related mutant, lacks the floorplate, and hence *twhh* expression, as *twhh* is only found in the floorplate (Rebagliati et al., 1998; Sampath et al., 1998).

In all three single mutants (*syu*, *cyc* or *ntl*) the ears are largely phenotypically normal, and show none of the defects found in *con* or *smu* embryos (data not shown). Although *cyc* homozygotes have slightly abnormally shaped ears, phalloidin staining reveals that the sensory patches are fully formed and present in the correct relative positions. *syu* mutant embryos, including the developing ear, are developmentally retarded. Otherwise, the ear appears normal, although the posterior macula may occasionally be positioned slightly too far towards the anterior. *ntl* ears appear normal in all respects. In all three single mutants, *nkx5.1* (an anterior marker), *folllistatin* (a posterior marker) and *bmp4* (a crista marker) are expressed normally (data not shown). The loss of function of each individual Hedgehog protein is therefore not sufficient to cause gross AP patterning defects in the developing ear.

To examine the ears of fish lacking function of two of the three Hedgehog proteins, we used double mutants and morpholino knockdowns (Nasevicius and Ekker, 2000;

Table 3. Summary of ear phenotypes caused by removal of function of one or more Hedgehog proteins via mutant analysis

Strain	Gene mutated	Hh removed	Ear defect
<i>syu</i> ^{td4}	<i>shh</i>	Shh	None*
<i>ntl</i> ^{tc41}	<i>brachyury</i>	Ehh	None
<i>cyc</i> ^{tf219}	<i>nodal</i> related	Twhh	None†
<i>syu</i> ^{td4} ; <i>ntl</i> ^{tc41}	<i>shh</i> ; <i>brachyury</i>	Shh; Ehh	None
<i>syu</i> ^{td4} ; <i>cyc</i> ^{tf219}	<i>shh</i> ; <i>nodal</i> related	Shh; Twhh	Anteriorised

*Developmentally retarded.
†Anteroposterior axis elongated with respect to dorsoventral axis.

Odenthal et al., 2000; Lewis and Eisen, 2001) (Tables 3 and 4). To remove functional *ehh* and *shh*, we crossed fish heterozygous for both *ntl* and *syu*. The ears of 137 live embryos from four clutches appeared morphologically normal, although some were developmentally retarded. As *ntl*;*syu* double homozygous embryos are difficult to distinguish from *ntl* homozygotes, all embryos displaying a *ntl* phenotype from three clutches (lacking a tail; *n*=19) were examined by phalloidin staining. In every case the sensory patches were well formed and positioned correctly, although in five fish, the presumed *ntl*;*syu* double mutants, the development of the sensory patches was retarded. These data indicate that removal of functional Ehh in addition to Shh is not sufficient to give a *con* or *smu*-like ear phenotype (Table 3 and data not shown).

By contrast, *cyc*;*syu* double homozygotes (identifiable

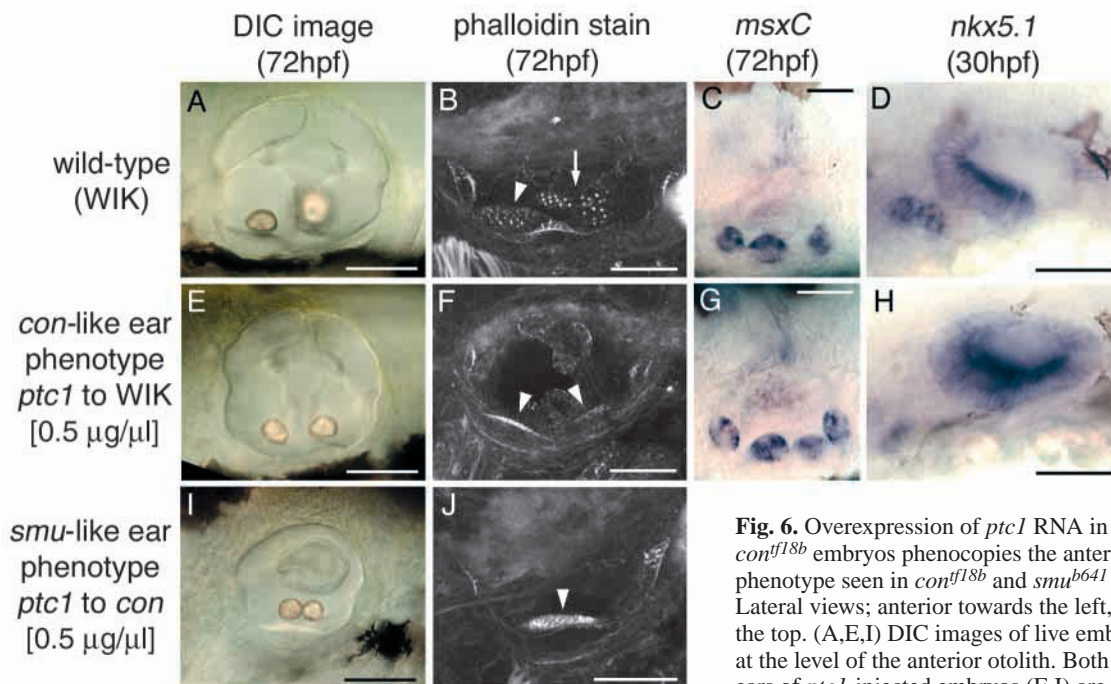


Fig. 6. Overexpression of *ptc1* RNA in wild-type and *con*^{f18b} embryos phenocopies the anteriorised ear phenotype seen in *con*^{f18b} and *smu*^{b641} homozygotes. Lateral views; anterior towards the left, dorsal towards the top. (A,E,I) DIC images of live embryos, focussed at the level of the anterior otolith. Both otoliths in the ears of *ptc1*-injected embryos (E,I) are small, lateral and ventral, and resemble the anterior otolith of wild-

type embryos (A). (B,F,J) Confocal images of FITC-phalloidin stained ears. (B) Wild-type pattern: arrowhead, anterior macula; arrow, posterior macula. A posterior macula is not present on the medial wall of *ptc1*-injected embryos (F,J). In ears of *ptc1* injected wild-type embryos, the anterior macula is present as normal but a second ventral macula is present at the posterior of the ear, as in *con* (arrowheads, F). In ears of *ptc1*-injected embryos from a *con*^{+/+} mating, a single ventral macula covers the ventral surface of the otic vesicle, as in *smu* ears (arrowhead, J). (C,D,G,H) In situ markers show similar expression patterns in the ears of *ptc1*-injected embryos and of *con* and *smu*. Four cristae may develop (G), and expression of the anterior marker *nkx5.1* is expanded (H). We do not have markers that distinguish between *con*-like and *smu*-like ears and so these assays were not repeated on *ptc1*-injected *con*^{f18b} embryos. Scale bars: 50 µm.

Table 4. Summary of ear phenotypes caused by injection of *twhh* and *shh* antisense morpholinos into one- or two-cell zebrafish embryos

Strain	Morpholino injected	Concentration (mM)	Hh removed	Number injected	Ear defect
WIK	<i>twhh</i> MO	0.25	Twhh	40	None
<i>syu</i> ^{t4} /+ × <i>syu</i> ^{t4} /+	<i>shh</i> MO	0.5	Shh	92*	None
<i>syu</i> ^{t4} /+ × <i>syu</i> ^{t4} /+	<i>twhh</i> MO	0.25	Shh + Twhh	174*	31 anteriorised/143 wild type

*Only 1/4 of these fish will be homozygous *syu*^{t4} mutants.

because they have both U-shaped somites and cyclopia) show an anteriorised ear phenotype similar to, but perhaps not quite as strong as, the *smu* phenotype. The posterior otolith is small and too lateral, resembling the anterior otolith (Fig. 7A,B); the

posterior macula is missing, and either a single macula covering the ventral surface of the ear (as in *smu*) or two separate ventral maculae (as in *con*) are seen (Fig. 7D,E). Additionally, anterior *nkx5.1* expression is expanded

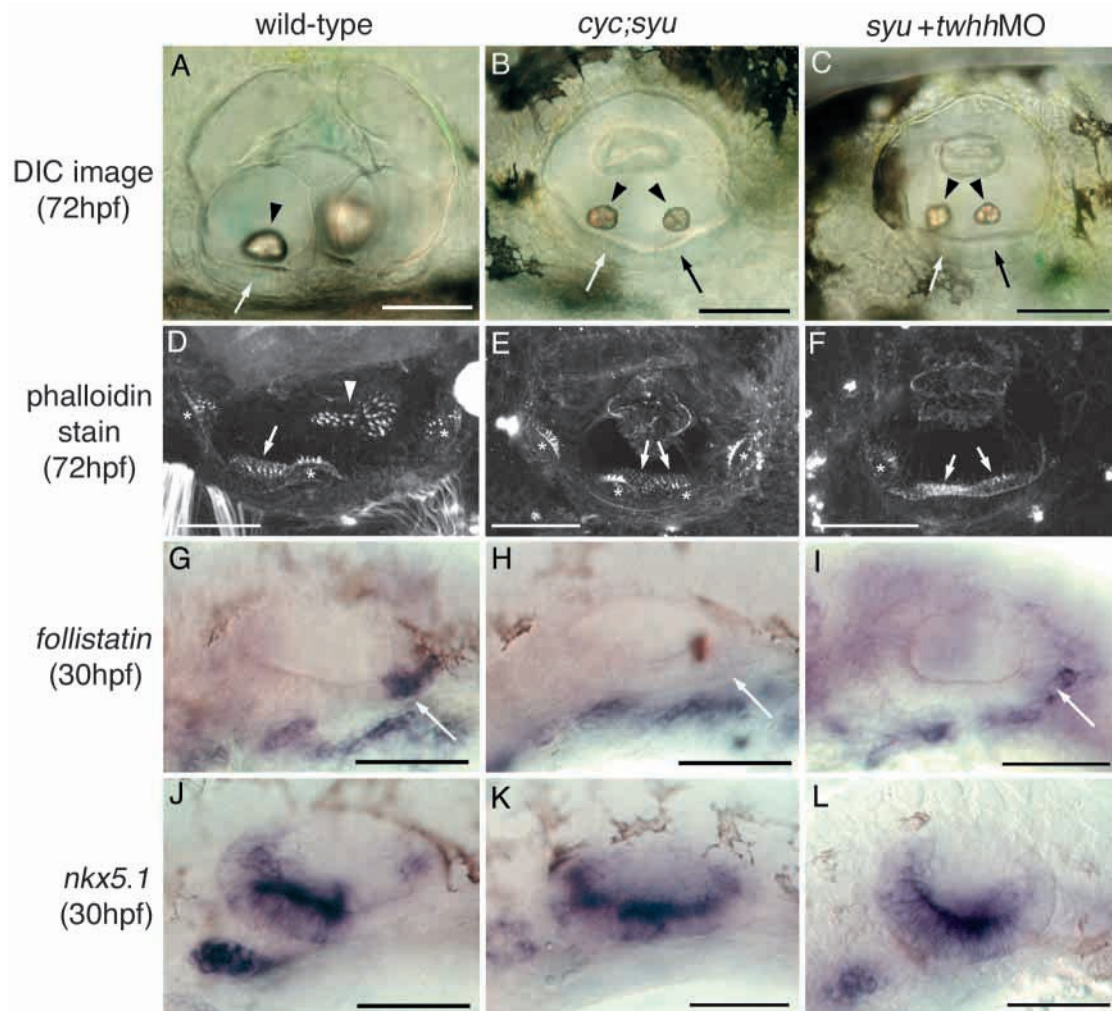


Fig. 7. Anteriorised ear phenotypes in *cyc;syu* double mutants and *twhh* antisense morpholino-injected *syu*^{t4} embryos. Lateral views; anterior towards the left, dorsal towards the top. (A,D,G,J) Wild-type ear pattern; A is taken from Fig. 3 for comparison. (B,E,H,K) Ears of *syu;cyu* double mutants. (C,F,I,L) Ears of *syu*^{t4} mutant embryos injected with 0.25mM *twhh* morpholino. (A-C) DIC images of live ears. The ears of *cyc;syu* mutants and *twhh* MO-injected embryos have two small, lateral otoliths (arrowheads B,C) resembling the anterior otolith of ears from wild-type embryos (arrowhead, A). Thickened sensory epithelium is present at both the anterior and the posterior of the vesicle in *cyc;syu* and *syu + twhh* MO embryos (arrows, B,C) rather than just at the anterior as in the wild-type (arrow, A). (D-F) Confocal images of FITC-phalloidin stains. Hair cells on the ventral floor are present at both the posterior and anterior of the vesicle in *cyc;syu* and *syu + twhh* MO embryos (arrows, E,F) rather than just at the anterior as in the wild-type (arrow, D). The posterior macula (arrowhead, D) is missing from the medial wall in *cyc;syu* and *syu + twhh* MO ears (E,F). Four cristae (*) rather than the usual three are present in some *cyc;syu* and *syu + twhh* MO embryos (e.g. E). Three cristae were present in the ear shown in F, but only one is in the focal plane. (G-L) In situ hybridisation. Arrows indicate the posterior domain of *follistatin* expression in the wild type (G). This is absent in *cyc;syu* and *syu + twhh* MO ears (H,I). Anterior *nkx5.1* expression (J) is expanded in *cyc;syu* and (less extensively) in *syu + twhh* MO ears (K,L). Scale bars: 50 μ m.

posteriorly and posterior *folliculin* expression is absent (Fig. 7G,H,I,K). *bmp4* expression indicated that four cristae instead of the usual three were present in 7/18 (38%) ears examined (data not shown). Removal of both *twhh* and *shh* function from the embryo is thus sufficient to cause anteriorisation of the otic vesicle, although removal of the function of either alone is not.

We confirmed this result by the use of antisense morpholinos to knock down Shh and Twhh function. Carboxyfluorescein-tagged antisense morpholinos were designed against *shh* and *twhh*, and injected into wild-type or *syu* mutant embryos. Injection of 0.25 mM *twhh* morpholino to wild-type (AB) embryos caused circulation defects and very slight somite defects. Although necrosis was observed in the head in some cases, the ears of all injected embryos developed normally (Table 4). To deplete both *twhh* and *shh* function, we injected 0.25 mM *twhh* MO into a clutch of embryos from a mating between *syu*+ parents. We observed a phenotype similar to that seen in *twhh* MO-injected wild-type embryos in 82% of cases. In the remaining 18% (the presumed *syu* homozygotes), the eyes were cyclopic and the ears resembled *con* and *smu* anteriorised ears. The otoliths both resembled the anterior otolith, a ventral sensory patch could be seen at the posterior of the ear and the posterior macula was absent (Fig. 7C,F). In addition, posterior otic *folliculin* expression was lost and anterior otic *nkx5.1* expression extended posteriorly, although not to the extent seen in *cyc;syu* double mutants (Fig. 7I,L).

As a control for nonspecific effects of *twhh* MO injection, we injected 0.5 mM *shh* MO into a clutch of embryos from a *syu*+ × *syu*+ mating. In no case was an anteriorised ear phenotype observed, although all embryos now resembled *syu* homozygotes in possessing circulation defects and U-shaped somites, confirming that our *shh* MO knocks down Shh function. These data indicate that the anteriorised ear phenotype seen in *twhh* MO-injected *syu* homozygotes is not due to nonspecific effects of morpholino injection (see Table 4). It therefore appears that both Twhh and Shh function to specify the posterior part of the ear, but that either can compensate for the absence of the other. We have not tested the role of Ehh with morpholinos, but suggest that it is unlikely to play a major role, given that the ears of *syu;ntl* double homozygotes, which lack both functional *shh* and *ehh*, are patterned normally.

Injection of *shh* or dnPKA RNA posteriorises the ears of wild-type embryos

As a loss of Hedgehog signalling leads to a loss of posterior character and a concomitant gain of anterior character at the posterior of the ear, we predicted that an increase in Hedgehog signalling should lead to a gain of posterior character by the

anterior part of the ear. We tested this hypothesis by overexpression of *shh* RNA or a dominant negative (dn) PKA RNA in wild-type embryos. We injected *shh* RNA into wild-type zebrafish embryos at concentrations of 25 ng/μl to 100 ng/μl. Approximately 65% of the ears of these embryos had a very small otic vesicle containing either a single central otolith or a fused dumb-bell shaped central otolith (Table 5; Fig. 8A-C). Semicircular canal projections were very reduced or absent in these ears (Fig. 8A-C). A few more weakly affected embryos displayed a variable semicircular canal phenotype where one or more of the canal projections was reduced or absent (data not shown). Phalloidin staining in those ears with a single or fused central otolith revealed the absence of an anterior macula and the presence of a single medial macula. This had a characteristic ‘bow-tie’ or ‘butterfly’ shape, and is presumed, based on its shape and position, to represent a twinned, double posterior macula (Fig. 8D-F). Increasing the concentration of RNA injected affects this phenotype. At 25 ng/μl, out of 15 posteriorised ears, ten showed the ‘bow-tie’ shape shown in Fig. 8F and five showed the ‘butterfly’ shape shown in Fig. 8E. At 100 ng/μl, out of six posteriorised ears, five showed the ‘butterfly’ phenotype, while one showed the ‘bow-tie’.

Phalloidin staining and in situ hybridisation with *msxc* also indicated that the cristae were variably reduced in the posteriorised ears. In most cases, all cristae were absent, but in a number of cases one or more were observed (data not shown). As before, we were unable to assign an identity to the cristae present. Anterior markers (*nkx5.1*, *pax5* and *fgf8*) were absent or severely reduced in 60% or more of cases (Fig. 8J-O), which is consistent with the number of ears with twinned posterior maculae in *shh*-injected embryos. *folliculin*, a posterior marker, was duplicated at the anterior in 5/22 ears examined or expanded anteriorly along the medial wall of the otic vesicle in 5/22 (Fig. 8G-I). These data suggest that the otic phenotype of *shh*-injected fish is indeed a posteriorisation of anterior otic regions. Injections of either *twhh* RNA or *ehh* RNA, at concentrations up to 500 ng/μl, had no effect on the otic vesicle.

A dominant-negative form of PKA (dnPKA) was also used to repress Hedgehog signalling activity. PKA acts downstream of Smo to repress Hh signalling and therefore dnPKA causes constitutive activation of the pathway (Concordet et al., 1996). dnPKA RNA (400 ng/μl) was injected into wild-type embryos, resulting in a phenotype identical to that caused by *shh* injections in 14% embryos (Fig. 8C,F). Lower concentrations had no effect on the otic vesicle. These data confirm that ectopic Hh activity can lead to a duplication of posterior structures at the expense of anterior domains.

Table 5. Ear phenotypes caused by injection of *shh* and dnPKA RNA into one- or two-cell zebrafish embryos

Strain injected	RNA injected	RNA concentration (ng)	Number in which there is no AP defect*	Number indistinct†	Single or fused otoliths	Total
WIK (wild-type)	<i>shh</i>	25	20 (33.3%)	4 (6.7%)	36 (60.0%)	60
WIK	<i>shh</i>	50	19 (41.3%)	0	27 (58.7%)	46
WIK	<i>shh</i>	100	6 (16%)	6 (16.7%)	24 (66.6%)	36
WIK	<i>shh</i>	100	5 (9.3%)	3 (5.5%)	46 (85.2%)	54
WIK	dnPKA	400	77 (58.3%)	36 (27.3%)	19 (14.4%)	132

*Based on otolith position and size. A variable crista and semicircular canal phenotype was seen in this group (not considered further in this report).

†Could not be clearly assigned to either category (e.g. otoliths small or too close together).

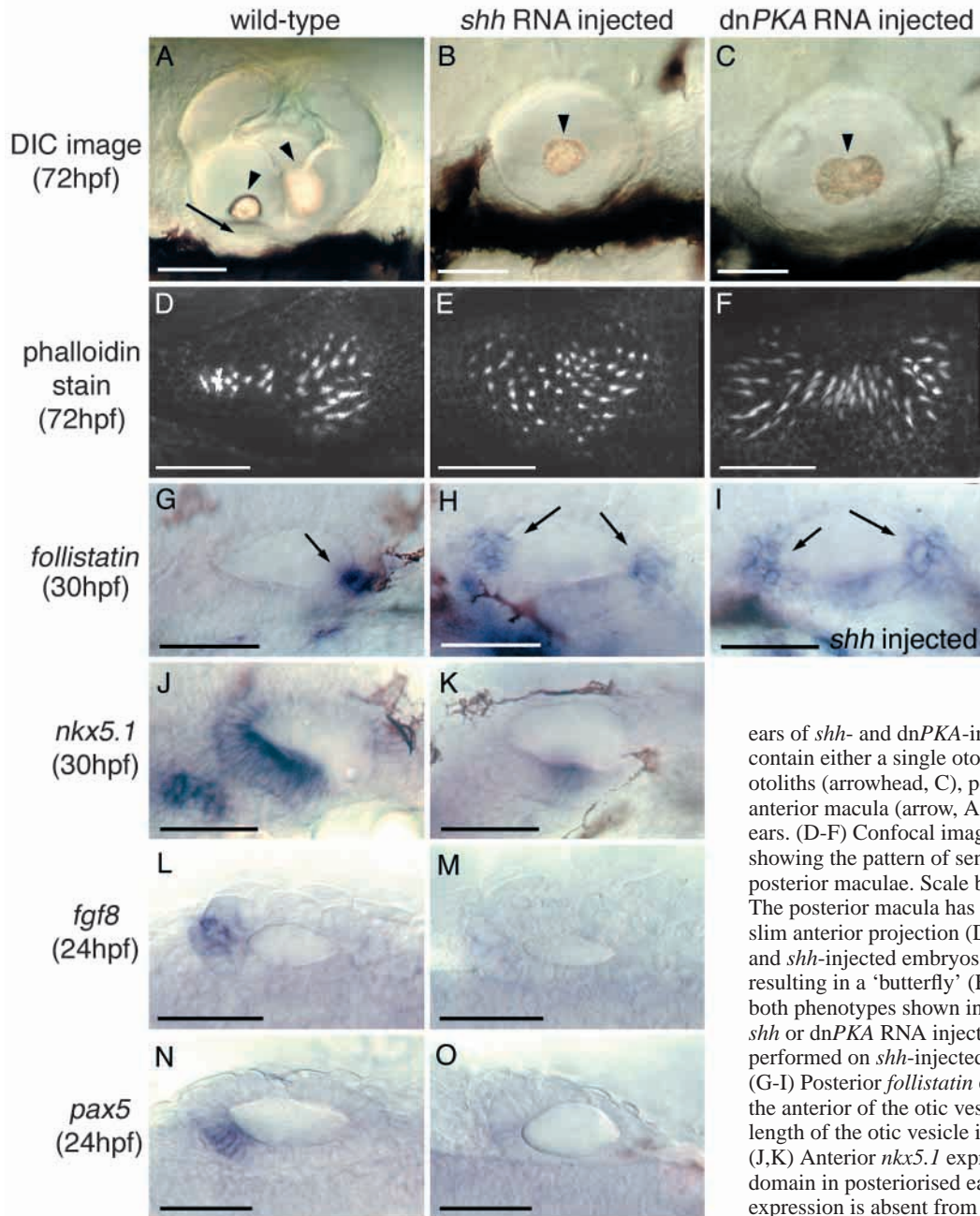


Fig. 8. Overexpression of *shh* and *dnPKA* RNA in wild-type embryos results in posteriorised ears. (A-K) Lateral views; anterior towards the left, dorsal towards the top. (L-O) Dorsal views; anterior towards the left, lateral towards the top. (A-C) DIC images of live ears. Scale bars: 50 µm. The

ears of *shh*- and *dnPKA*-injected embryos are small and contain either a single otolith (arrowhead, B) or fused otoliths (arrowhead, C), positioned medially. A ventral anterior macula (arrow, A) is absent in these posteriorised ears. (D-F) Confocal images of FITC-phalloidin stains showing the pattern of sensory hair cell stereocilia in posterior maculae. Scale bars: 25 µm. (D) Wild-type pattern. The posterior macula has a rounded posterior region and a slim anterior projection (D). Posterior maculae of *dnPKA*- and *shh*-injected embryos have two rounded posterior ends resulting in a 'butterfly' (E) or 'bow-tie' (F) shape. Note that both phenotypes shown in B,C,E,F could be caused by either *shh* or *dnPKA* RNA injection. (G-O) In situ hybridisation performed on *shh*-injected embryos. Scale bars: 50 µm. (G-I) Posterior *follistatin* expression is either duplicated at the anterior of the otic vesicle or extends medially along the length of the otic vesicle in posteriorised ears (arrows). (J,K) Anterior *nkx5.1* expression is reduced to a small central domain in posteriorised ears. (L-O) Anterior *fgf8* and *pax5* expression is absent from posteriorised ears.

DISCUSSION

In this study, we have examined the role of signalling molecules of the Hedgehog (Hh) family in patterning the axes of the zebrafish otic vesicle. The closest sources of Hh protein to the developing ear are ventral midline structures (notochord and floorplate). As these are situated ventral and medial to the otic vesicles, we predicted that Hh would have a mediolateral (ML) or dorsoventral (DV) patterning role in the developing ear. However, we found that both the ML and DV axes of the ear appeared to be patterned correctly in the absence of Hh signalling. Instead, our data indicate that both *Shh* and *Twhh* have a role in specifying posterior otic structures. Severely reduced or absent Hh signalling leads to a loss of posterior otic

structures and a concomitant partial mirror image duplication of anterior regions. Increased Hh signalling throughout the embryo leads to the reverse phenotype: a loss of anterior otic structures and a mirror image duplication of posterior regions.

Based on the expression of *ptc1* and *ptc2* in the ears of wild-type embryos, *con* and *smu* mutants, and embryos overexpressing *shh* RNA, we argue that the effect of Hh signalling on the ear is likely to be direct. However, we cannot rule out the possibility that Hh acts in a permissive manner on surrounding tissues to potentiate or block the production or action of a localised factor, which then acts secondarily to pattern the ear. We find no evidence, however, that AP pattern in the hindbrain is altered in embryos with attenuated Hh signalling: AP expression of *krx20* (*egr2* – Zebrafish

Information Network) *hoxb4a* and *val/mafb*, for example, is normal in the rhombomeres of *con* mutants (data not shown).

The inner ear phenotype of mice homozygous for a mutation in the *shh* gene has recently been reported (Liu et al., 2002; Riccomagno et al., 2002). The defects do not appear to mimic those we see in *smu* or *con*, but they primarily affect structures that have no direct counterpart in the fish ear. In particular, the cochlear duct and cochleovestibular ganglia, all ventral otic derivatives, are rudimentary or absent, and *Pax2* expression is diminished in the vesicle; by contrast, in *smu* and *con* mutants, specification of otic neuroblasts does occur, and otic *pax2a* expression is retained (Fig. 4; data not shown). Note that in the mouse, inactivation of *Shh* gives rise to much more severe overall head defects than in any of the zebrafish Hh pathway mutants, characterised by holoprosencephaly and cyclopia (Chiang et al., 1996). In vitro and in vivo evidence also suggests a later role for Shh in chondrogenesis of the murine otic capsule (Liu et al., 2002; Riccomagno et al., 2002).

Hh signalling may act to pattern the otic epithelium at or soon after vesicle formation

Although our experiments do not address the timing of Hh action rigorously, we suggest that the zebrafish ear is likely to respond to Hh signalling between 19 and 24 hpf. Exogenous RNA injected at the one- to two-cell stage and protein translated from it are likely to degrade before 24 hpf (Hammerschmidt et al., 1999) (K. L. H., unpublished), but injection of *ptc1* RNA is sufficient to repress endogenous Hh signalling and phenocopy the defects seen in *smu* and *con*. Hh may not, however, exert its posterior inductive abilities as early as 16–17.5 hpf, when the earliest AP molecular asymmetries appear (*nkx5.1* and *pax5* expression) (Pfeffer et al., 1998; Adamska et al., 2000). This is because Hh signalling activity, as indicated by the expression of its target gene *ptc1*, only becomes concentrated in posterior otic epithelium between 19 hpf and 22 hpf. Before this, *ptc1* expression (and hence Hh activity) is detectable in a ventromedial domain along the entire AP length of the otic vesicle.

If Hh does act prior to 19 hpf, it is possible that ventromedial cells specified by Hh later move to occupy more posterior positions, thus transforming a DV or ML signal into an AP pattern. Although a fate map of the zebrafish otic vesicle exists (Haddon, 1997), it is not sufficiently detailed to tell whether such movements do generally occur. Grafting experiments in salamander embryos are suggestive of an anterior to posterior movement of ventromedial otic cells (Kaan, 1926), but species-specific differences are likely: in the chick otic cup, ventral cells tend to move in an anterodorsal direction (Brigande et al., 2000a). In addition, amphibian ears may show a high degree of cell mixing (Kil and Collazo, 2001), but this appears to be more limited in the zebrafish and chick otic vesicle (Haddon, 1997; Brigande et al., 2000a).

Alternatively, Hh may act after 19 hpf to reinforce and maintain AP polarity in the ear rather than establish it, in a similar fashion to the role of Hh in the vertebrate limb bud. Here, Shh expression in the zone of polarising activity (ZPA) is established by a prepattern involving mutual antagonism between the transcription factors GLI3 and dHAND (te Welscher et al., 2002). In the zebrafish fin bud, for example, a transient AP polarity is established (but not maintained) in the fin buds of *syu* (*shh*) mutants (Neumann et al., 1999), but no

AP patterning is ever apparent in the fin buds of *hands off* (*hand2*) mutants (Yelon et al., 2000).

Hh signalling appears to affect the ear in a dose-dependent manner

Only a low level of Hh signalling is required for correct patterning of the zebrafish otic vesicle; defects are evident only in those mutants with the strongest phenotypes in other tissues (*smu* and *con*), or when the activity of both Shh and Twhh are removed. The ears are also patterned correctly in *ntl*, *fth* and *oep* embryos, in which the development of subsets of tissues expressing Hh is compromised (data not shown; see below). Despite this, we observe phenotypes that appear to differ according to the level of Hh activity. The anterior duplication is incomplete in both *smu* and *con* ears, but the *smu* phenotype appears to be stronger; we see a single fused ventral macula rather than the two separate ventral maculae found in *con*. This correlates with the fact that *smu* homozygotes show a more complete loss of Hh signalling than *con* homozygotes (Lewis et al., 1999b; Barresi et al., 2000; Varga et al., 2001). Moreover, the different otic defects can be phenocopied by different levels of Hh inhibition via *ptc1* injection. We also observe a dose-dependent effect of Shh or dnPKA injection; low doses more frequently result in a 'bow-tie'-shaped posterior macula, whereas higher doses (100 ng) more frequently result in the 'butterfly' phenotype.

Other mirror image duplications

The ears described in this work are enantiomorphic twins: they consist of two mirror image halves. Mirror image duplications of various tissues have been observed in several other contexts, and are frequently associated with alterations of Hh signalling. Examples include the development of adult abdominal segments and the wing in *Drosophila* (Basler and Struhl, 1994; Capdevila and Guerrero, 1994; Kojima et al., 1994; Kopp et al., 1997; Struhl et al., 1997a; Struhl et al., 1997b; Lawrence et al., 2002), and development of the limb bud in vertebrates (Riddle et al., 1993; Yang et al., 1997). Mutants for *hh*, *ci* and *ptc* in *Drosophila* are themselves members of the segment polarity class, in which a proportion of each embryonic abdominal segment is deleted and the remainder present as a mirror image duplication (Nüsslein-Volhard and Wieschaus, 1980).

Mirror image duplications of the inner ear have also been documented previously. Harrison transplanted ear rudiments in salamander (*Amblystoma*) embryos such that their AP axis was reversed with respect to that of the host (Harrison, 1936; Harrison, 1945). Ear rudiments transplanted early (at the neural plate stage) developed with an AP axis corresponding to that of the host, while ear rudiments transplanted later (after closure of the neural folds) developed according to the donor AP axis. However, in transplantations performed at intermediate stages (during neural tube closure; stage 19–21), up to 27% of transplanted ear rudiments developed as mirror image twins. These ears consisted of two posterior halves, two anterior halves or incomplete duplications, and show a remarkable similarity to the zebrafish phenotypes we describe. In the double anterior ears, four cristae and two utricular maculae and otoliths were observed; in the double posterior ears, utricular maculae were missing, and cristae were reduced (Harrison, 1936; Harrison, 1945). Similar duplications have been

observed in *Xenopus* embryos after ablation of either the anterior or posterior half of the otic placode. Regeneration after anterior ablations results in mirror image double posterior ears, while posterior ablations can cause the reverse phenotype (Waldman et al., 2001).

Restriction of Hh activity to the posterior of the ear

In the above examples involving Hh, a localised source of Hh provides the necessary information to generate AP polarity. In most cases this is either a point source (as in the vertebrate limb bud) or a linear boundary (as in the fly wing disc). However, in the fish ear, the strongest and closest source of Hh appears to be constant along the AP axis. It is possible that endodermal expression of Shh influences the ear, but we think this unlikely, given its late onset. Unless Hh-receiving cells move to the posterior of the ear (as discussed above), a mechanism must exist to restrict the effects of Hh activity to the posterior of the ear.

One possibility is that posterior otic regions receive more Hh than anterior domains because of positioning of the otic vesicle relative to the midline and the notochord. At 22 hpf, when active Hh signalling is first concentrated in posterior otic epithelium, anterior otic regions are a little further from the midline than posterior regions (see Fig. 1J). Although slight, this difference may play some part in the concentration of higher level Hh activity in posterior otic regions. In addition, the anterior limit of the notochord coincides roughly with the anterior limit of the otic vesicle (Fig. 9), and thus notochord-derived Hh may be reduced at the anterior of the vesicle. We have found, however, that either the notochord or the floorplate alone suffices to pattern the ear correctly. The ears of *ntl* mutants, which lack a notochord (Schulte-Merker et al., 1994), *flh* mutants, which lack chordamesoderm (Halpern et al., 1995), and *cyc* and *oep* mutants, both of which lack a medial floorplate (Schier et al., 1997; Rebagliati et al., 1998), all show correct AP patterning (data not shown). Assuming that post-transcriptional and post-translational processing, release and diffusion of Hh are equivalent at different AP levels in the otic region, it appears that a constant source of Hh from midline tissues, encoded by *twhh* or *shh*, is able to pattern posterior regions of the ear.

If the source of Hh is constant, it is likely that other factors, originating either from within or outside the otic vesicle, synergise with Hh in posterior regions or antagonise it at the anterior (Fig. 9). Members of the bone morphogenetic protein (BMP), BMP antagonist, Wnt and fibroblast growth factor (FGF) families are good candidates for such factors, as they are known to potentiate or antagonise Hh in many developmental contexts (see Marcelle et al., 1997; Meyers and Martin, 1999; Patten and Placzek, 2002) (reviewed by Cohn and Tickle, 1996; McMahon et al., 2003). Members of all four families are expressed in the developing zebrafish ear (Blader et al., 1996; Reifers et al., 1998; Mowbray et al., 2001).

Among the best candidates for antagonists of Hh activity in anterior otic epithelium are Fgf3 and Fgf8. Both have an early role in otic placode induction: disruption of the function of either Fgf results in a small otic placode, and if both are disrupted the otic placode is severely reduced or fails to form entirely (Phillips et al., 2001; Raible and Brand, 2001; Maroon et al., 2002). Later, at the stages when Hh is likely to be active, *fgf3* continues to be expressed in r4 (now positioned adjacent

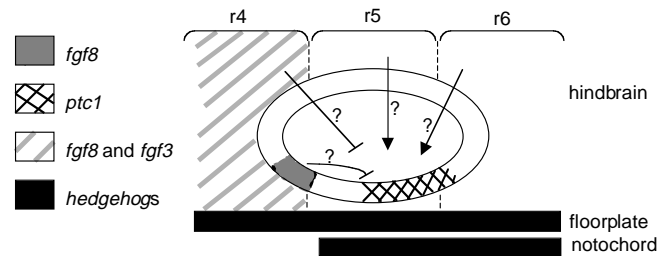


Fig. 9. Hindbrain- or otic vesicle-derived factors may concentrate Hh signalling activity in posterior otic epithelium. Schematic of a zebrafish otic vesicle and surrounding tissues during late somitogenesis stages, showing the expression domains of potential Hh-interacting factors and of *hh* and *ptc1*. Lateral view; anterior towards the left, dorsal towards the top. r4/5/6, rhombomere 4/5/6 of the hindbrain. Factors from r4 of the hindbrain or anterior otic epithelium, e.g. Fgf3 and Fgf8, may repress *ptc1* expression and hence Hh activity at the anterior of the otic vesicle. Alternatively, or in addition, factors from r5/6 or the posterior otic vesicle may potentiate Hh signalling activity and hence *ptc1* expression at the posterior of the vesicle.

to the anterior part of the otic vesicle), while *fgf8* is expressed in the anterior otic epithelium (Fig. 4M) (Reifers et al., 1998; Phillips et al., 2001; Maroon et al., 2002). Both factors appear to have anterior otic inducing ability. In *valentino* (*mafB*) embryos, hindbrain *fgf3* expression is expanded posteriorly, resulting in the expansion of anterior-specific gene expression in the ear. Conversely, in embryos where Fgf3 function is depleted by morpholino injection, expression of some anterior-specific otic genes is reduced or missing (Kwak et al., 2002). In the *acerebellar* (*fgf8*) mutant, *nkx5.1* expression is reduced, suggesting that some loss of anterior character has occurred (Adamska et al., 2000). Thus Fgf3 from the hindbrain and Fgf8 in the otic epithelium are excellent candidates for antagonists of Hh activity in the anterior otic vesicle (Fig. 9).

Conclusion

In all likelihood, more than one mechanism operates to concentrate Hh activity in posterior regions of the otic vesicle. Whichever mechanism is responsible, it is clear that Hh is essential for the specification of posterior otic identity in the zebrafish. We still do not understand, however, how this is effected. The mirror image duplications observed appear to reveal an underlying prepattern, where the otic vesicle is an equipotential system in which the two ends (or the centre) are specified, but an A or P identity has not been assigned to either. This is similar to the 'global mirror-symmetric system' proposed for the *Drosophila* adult abdominal segment by Kopp and Duncan (Kopp and Duncan, 1997). We note that the early expression of genes marking the positions of the presumptive maculae at the two ends of the otic vesicle, such as the Delta genes, is initially mirror symmetric (Haddon et al., 1998). A symmetric prepattern would then be acted on by Hh, Fgf and other signals, from surrounding tissues and within the ear, to establish and maintain AP polarity.

We thank J. Lewis for inspiration, A. Jamieson for help with a pilot study (funded by a Nuffield Foundation vacation studentship), P. Ingham, S. Roy, C. Wolff and J. Begbie for helpful discussion, S. Roy and C. Wolff for help with establishment of stocks, and F. Wilson and

L. Gleadall for care of the fish facility. We are grateful to R. Karlstrom and B. Riley for communicating data before publication, and many members of the zebrafish community for supplying cDNAs. This work was supported by a Wellcome Trust project grant (057101). Support for confocal microscopy was provided by Yorkshire Cancer Research.

REFERENCES

- Adamska, M., Léger, S., Brand, M., Hadrys, T., Braun, T. and Bober, E. (2000). Inner ear and lateral line expression of a zebrafish *Nkx5-1* gene and its downregulation in the ears of FGF8 mutant, *ace*. *Mech. Dev.* **97**, 161-165.
- Akimenko, M.-A., Ekker, M., Wegner, J., Lin, W. and Westerfield, M. (1994). Combinatorial expression of three zebrafish genes related to *Distal-Less*: Part of a homeobox gene code for the head. *J. Neurosci.* **14**, 3475-3486.
- Barresi, M. J., Stickney, H. L. and Devoto, S. H. (2000). The zebrafish slow muscle omitted gene product is required for Hedgehog signal transduction and the development of slow muscle identity. *Development* **127**, 3475-3486.
- Basler, K. and Struhl, G. (1994). Compartment boundaries and the control of *Drosophila* limb pattern by *hedgehog* protein. *Nature* **368**, 208-214.
- Blader, P., Strähle, U. and Ingham, P. W. (1996). Three Wnt genes expressed in a wide variety of tissues during development of the zebrafish, *Danio rerio*: developmental and evolutionary perspectives. *Dev. Genes Evol.* **206**, 3-13.
- Brigande, J. V., Iten, L. E. and Fekete, D. M. (2000a). A fate map of chick otic cup closure reveals lineage boundaries in the dorsal otocyst. *Dev. Biol.* **227**, 256-270.
- Brigande, J. V., Kiernan, A. E., Gao, X., Iten, L. E. and Fekete, D. M. (2000b). Molecular genetics of pattern formation in the inner ear: Do compartment boundaries play a role? *Proc. Natl. Acad. Sci. USA* **97**, 11700-11706.
- Capdevila, J. and Guerrero, I. (1994). Targeted expression of the signaling molecule decapentaplegic induces pattern duplications and growth alterations in *Drosophila* wings. *EMBO J.* **13**, 4459-4468.
- Chen, W., Burgess, S. and Hopkins, N. (2001). Analysis of the zebrafish *smoothened* mutant reveals conserved and divergent functions of Hedgehog activity. *Development* **128**, 2385-2396.
- Chiang, C., Litingtung, Y., Lee, E., Young, K. E., Corden, J. L., Westphal, H. and Beachy, P. A. (1996). Cyclopia and defective axial patterning in mice lacking *Sonic hedgehog* gene function. *Nature* **383**, 407-413.
- Cohn, M. and Tickle, C. (1996). Limbs: a model for pattern formation within the vertebrate body plan. *Trends Genet.* **12**, 253-257.
- Concordet, J. P., Lewis, K. E., Moore, J. W., Goodrich, L. V., Johnson, R. L., Scott, M. P. and Ingham, P. W. (1996). Spatial regulation of a zebrafish *patched* homologue reflects the roles of *sonic hedgehog* and *protein kinase A* in neural tube and somite patterning. *Development* **122**, 2835-2846.
- Currie, P. D. and Ingham, P. W. (1996). Induction of a specific muscle cell type by a hedgehog-like protein in zebrafish. *Nature* **382**, 452-455.
- Deol, M. S. (1964). The abnormalities of the inner ear in *kreisler* mice. *J. Embryol. Exp. Morphol.* **12**, 475-490.
- Echelard, Y., Epstein, D. J., St-Jacques, B., Shen, L., Mohler, J., McMahon, J. A. and McMahon, A. P. (1993). Sonic hedgehog, a member of a family of putative signaling molecules, is implicated in the regulation of CNS polarity. *Cell* **75**, 1417-1430.
- Ekker, S. C., Ungar, A. R., Greenstein, P., von Kessler, D. P., Porter, J. A., Moon, R. T. and Beachy, P. A. (1995). Patterning activities of vertebrate *hedgehog* proteins in the developing eye and brain. *Curr. Biol.* **5**, 944-955.
- Ekker, M., Akimenko, M.-A., Allende, M. L., Smith, R., Drouin, G., Langille, R. M., Weinberg, E. S. and Westerfield, M. (1997). Relationships among *msx* gene structure and function in zebrafish and other vertebrates. *Mol. Biol. Evol.* **14**, 1008-1022.
- Fekete, D. M. (1996). Cell fate specification in the inner ear. *Curr. Opin. Neurobiol.* **6**, 533-541.
- Giraldez, F. (1998). Regionalized organizing activity of the neural tube revealed by the regulation of *lmx1* in the otic vesicle. *Dev. Biol.* **203**, 189-200.
- Goodrich, L. V., Johnson, R. L., Milenkovic, L., McMahon, J. A. and Scott, M. P. (1996). Conservation of the hedgehog/patched signaling pathway from flies to mice: induction of a mouse *patched* gene by Hedgehog. *Genes Dev.* **10**, 301-312.
- Goodrich, L. V., Jung, D., Higgins, K. M. and Scott, M. P. (1999). Overexpression of *ptcl* inhibits induction of Shh target genes and prevents normal patterning in the neural tube. *Dev. Biol.* **211**, 323-334.
- Gritli-Linde, A., Lewis, P., McMahon, A. P. and Linde, A. (2001). The whereabouts of a morphogen: direct evidence for short- and graded long-range activity of hedgehog signaling peptides. *Dev. Biol.* **236**, 364-386.
- Haddon, C. M. (1997). The development of the zebrafish ear and a quest for genes involved in sensory patterning. PhD Thesis, The Open University.
- Haddon, C. and Lewis, J. (1996). Early ear development in the embryo of the zebrafish, *Danio rerio*. *J. Comp. Neurol.* **365**, 113-123.
- Haddon, C., Jiang, Y.-J., Smithers, L. and Lewis, J. (1998). Delta-Notch signalling and the patterning of sensory cell differentiation in the zebrafish ear: evidence from the *mind bomb* mutant. *Development* **125**, 4637-4644.
- Halpern, M. E., Thisse, C., Ho, R. K., Thisse, B., Riggleman, B., Trevarrow, B., Weinberg, E. S., Postlethwait, J. H. and Kimmel, C. B. (1995). Cell-autonomous shift from axial to paraxial mesodermal development in zebrafish *floating head* mutants. *Development* **121**, 4257-4264.
- Hammerschmidt, M., Brook, A. and McMahon, A. P. (1997). The world according to *hedgehog*. *Trends Genet.* **13**, 14-21.
- Hammerschmidt, M., Blader, P. and Strähle, U. (1999). Strategies to perturb zebrafish development. *Meth. Cell Biol.* **59**, 87-115.
- Hammond, K., Hill, R., Whitfield, T. T. and Currie, P. (2002). Isolation of three zebrafish *dachshund* homologues and their expression in sensory organs, the central nervous system and pectoral fin buds. *Mech. Dev.* **112**, 183-189.
- Harrison, R. G. (1936). Relations of symmetry in the developing ear of *Amblystoma punctatum*. *Proc. Natl. Acad. Sci. USA* **22**, 238-247.
- Harrison, R. G. (1945). Relations of symmetry in the developing embryo. *Trans. Conn. Acad. Arts Sci.* **36**, 277-330.
- Ingham, P. W. and McMahon, A. P. (2001). Hedgehog signaling in animal development: paradigms and principles. *Genes Dev.* **15**, 3059-3087.
- Kaan, H. W. (1926). Experiments on the development of the ear of *Amblystoma punctatum*. *J. Exp. Zool.* **46**, 13-61.
- Karlstrom, R. O., Talbot, W. S. and Schier, A. F. (1999). Comparative synteny cloning of zebrafish *you-too*: mutations in the Hedgehog target *gli2* affect ventral forebrain patterning. *Genes Dev.* **13**, 388-393.
- Karlstrom, R. O., Tyurina, O., Kawakami, A., Nishioka, N., Talbot, W. S., Sasaki, H. and Schier, A. F. (2003). Genetic analysis of zebrafish *gli1* and *gli2* reveals divergent requirements for *gli* genes in vertebrate development. *Development* (in press).
- Kil, S.-H. and Collazo, A. (2001). Origins of inner ear sensory organs revealed by fate map and time-lapse analyses. *Dev. Biol.* **233**, 365-379.
- Kimmel, C. B., Ballard, W. W., Kimmel, S. R., Ullmann, B. and Schilling, T. F. (1995). Stages of embryonic development of the zebrafish. *Dev. Dyn.* **203**, 253-310.
- Kojima, T., Michiue, T., Orihara, M. and Saigo, K. (1994). Induction of a mirror-image duplication of anterior wing structures by localized *hedgehog* expression in the anterior compartment of *Drosophila melanogaster* wing imaginal discs. *Gene* **148**, 211-217.
- Kopp, A. and Duncan, I. (1997). Control of cell fate and polarity in the adult abdominal segments of *Drosophila* by *optomotor-blind*. *Development* **124**, 3715-3726.
- Kopp, A., Muskavitch, M. A. and Duncan, I. (1997). The roles of *hedgehog* and *engrailed* in patterning adult abdominal segments of *Drosophila*. *Development* **124**, 3703-3714.
- Krauss, S., Johansen, T., Korzh, V. and Fjose, A. (1991). Expression of the zebrafish paired box gene *pax[*zfb*]* during early neurogenesis. *Development* **113**, 1193-1206.
- Krauss, S., Concordet, J.-P. and Ingham, P. W. (1993). A functionally conserved homolog of the *Drosophila* segment polarity gene *hedgehog* is expressed in tissues with polarizing activity in zebrafish embryos. *Cell* **75**, 1431-1444.
- Krieg, P. A. and Melton, D. A. (1984). Functional messenger RNAs are produced by SP6 in vitro transcription of cloned cDNAs. *Nucleic Acids Res.* **12**, 7057-7070.
- Kwak, S.-J., Phillips, B. T., Heck, R. and Riley, B. B. (2002). An expanded domain of *fgf3* expression in the hindbrain of zebrafish *valentino* mutants results in mis-patterning of the otic vesicle. *Development* **129**, 5279-5287.
- Lawrence, P. A., Casal, J. and Struhl, G. (2002). Towards a model of the organisation of planar polarity and pattern in the *Drosophila* abdomen. *Development* **129**, 2749-2760.
- Lewis, K. E., Concordet, J. P. and Ingham, P. W. (1999a). Characterisation of a second *patched* gene in the zebrafish *Danio rerio* and the differential response of *patched* genes to Hedgehog signalling. *Dev. Biol.* **208**, 14-29.

- Lewis, K. E., Currie, P. D., Roy, S., Schauerte, H., Haffter, P. and Ingham, P. W. (1999b). Control of muscle cell-type specification in the zebrafish embryo by Hedgehog signalling. *Dev. Biol.* **216**, 469-480.
- Lewis, K. E. and Eisen, J. S. (2001). Hedgehog signaling is required for primary motoneuron induction in zebrafish. *Development* **128**, 3485-3495.
- Lewis, P. M., Dunn, M. P., McMahon, J. A., Logan, M., Martin, J. F., St-Jacques, B. and McMahon, A. P. (2001). Cholesterol modification of sonic hedgehog is required for long-range signaling activity and effective modulation of signaling by Ptc1. *Cell* **105**, 599-612.
- Liu, W., Li, G., Chien, J. S., Raft, S., Zhang, H., Chiang, C. and Frenz, D. A. (2002). Sonic hedgehog regulates otic capsule chondrogenesis and inner ear development in the mouse embryo. *Dev. Biol.* **248**, 240-250.
- Mansour, S. L., Goddard, J. M. and Capecchi, M. R. (1993). Mice homozygous for a targeted disruption of the proto-oncogene *int-2* have developmental defects in the tail and inner ear. *Development* **117**, 13-28.
- Marcelle, C., Stark, M. R. and Bronner-Fraser, M. (1997). Coordinate actions of BMPs, Wnts, Shh and noggin mediate patterning of the dorsal somite. *Development* **124**, 3955-3963.
- Mark, M., Lufkin, T., Vonesch, J.-L., Ruberte, E., Olivo, J.-C., Dollé, P., Gorry, P., Lumsden, A. and Chambon, P. (1993). Two rhombomeres are altered in Hoxa-1 mutant mice. *Development* **119**, 319-338.
- Maroon, H., Walshe, J., Mahmood, R., Kiefer, P., Dickson, C. and Mason, I. (2002). Fgf3 and Fgf8 are required together for formation of the otic placode and vesicle. *Development* **129**, 2099-2108.
- McKay, I. J., Lewis, J. and Lumsden, A. (1996). The role of FGF-3 in early inner ear development: An analysis in normal and *kreisler* mutant mice. *Dev. Biol.* **174**, 370-378.
- McMahon, A. P., Ingham, P. W. and Tabin, C. (2003). Developmental roles and clinical significance of Hedgehog signaling. *Curr. Top. Dev. Biol.* **53**, 1-114.
- Meyers, E. N. and Martin, G. R. (1999). Differences in left-right axis pathways in mouse and chick: functions of FGF8 and SHH. *Science* **285**, 403-405.
- Mowbray, C., Hammerschmidt, M. and Whitfield, T. T. (2001). Expression of BMP signalling pathway members in the developing zebrafish inner ear and lateral line. *Mech. Dev.* **108**, 179-184.
- Nasevicius, A. and Ekker, S. C. (2000). Effective targeted gene 'knockdown' in zebrafish. *Nat. Genet.* **26**, 216-220.
- Neumann, C. J., Grandel, H., Gaffield, W., Schulte-Merker, S. and Nüsslein-Volhard, C. (1999). Transient establishment of anteroposterior polarity in the zebrafish pectoral fin bud in the absence of sonic hedgehog activity. *Development* **126**, 4817-4826.
- Niederreither, K., Vermot, J., Schubaur, B., Chambon, P. and Dollé, P. (2000). Retinoic acid synthesis and hindbrain patterning in the mouse embryo. *Development* **127**, 75-85.
- Nüsslein-Volhard, C. and Wieschaus, E. (1980). Mutations affecting segment number and polarity in *Drosophila*. *Nature* **287**, 795-801.
- Odenthal, J., van Eeden, F. J., Haffter, P., Ingham, P. W. and Nüsslein-Volhard, C. (2000). Two distinct cell populations in the floor plate of the zebrafish are induced by different pathways. *Dev. Biol.* **219**, 350-363.
- Oxtoby, E. and Jowett, T. (1993). Cloning of the zebrafish *krox-20* gene (*krx-20*) and its expression during hindbrain development. *Nucleic Acids Res.* **21**, 1087-1095.
- Patten, I. and Placzek, M. (2002). Opponent activities of Shh and BMP signaling during floor plate induction in vivo. *Curr. Biol.* **12**, 47-52.
- Pfeffer, P. L., Gerster, T., Lun, K., Brand, M. and Busslinger, M. (1998). Characterization of three novel members of the zebrafish *Pax2/5/8* family: dependency of *Pax5* and *Pax8* expression on the *Pax2.1* (*noi*) function. *Development* **125**, 3063-3074.
- Phillips, B. T., Bolding, K. and Riley, B. B. (2001). Zebrafish *fgf3* and *fgf8* encode redundant functions required for otic placode induction. *Dev. Biol.* **235**, 351-365.
- Piotrowski, T. and Nüsslein-Volhard, C. (2000). The endoderm plays an important role in patterning the segmented pharyngeal region in zebrafish (*Danio rerio*). *Dev. Biol.* **225**, 339-356.
- Prince, V. E., Moens, C. B., Kimmel, C. B. and Ho, R. K. (1998). Zebrafish *hox* genes: expression in the hindbrain region of wild-type and mutants of the segmentation gene, *valentino*. *Development* **125**, 393-406.
- Raible, F. and Brand, M. (2001). Tight transcriptional control of the ETS domain factors *Erm* and *Pea3* by Fgf signaling during early zebrafish development. *Mech. Dev.* **107**, 105-117.
- Rebagliati, M. R., Toyama, R., Haffter, P. and Dawid, I. B. (1998). *cyclops* encodes a nodal-related factor involved in midline signaling. *Proc. Natl. Acad. Sci. USA* **95**, 9932-9937.
- Reifers, F., Böhli, H., Walsh, E. C., Crossley, P. H., Stainier, D. Y. R. and Brand, M. (1998). *Fgf8* is mutated in zebrafish *acerebellar* (*ace*) mutants and is required for maintenance of midbrain-hindbrain boundary development and somitogenesis. *Development* **125**, 2381-2396.
- Riccomagno, M. M., Martinu, L., Mulheisen, M., Wu, D. K. and Epstein, D. J. (2002). Specification of the mammalian cochlea is dependent on Sonic hedgehog. *Genes Dev.* **16**, 2365-2378.
- Riddle, R. D., Johnson, R. L., Laufer, E. and Tabin, C. (1993). Sonic hedgehog mediates the polarizing activity of the ZPA. *Cell* **75**, 1401-1416.
- Roelink, H., Porter, J. A., Chiang, C., Tanabe, Y., Chang, D. T., Beachy, P. A. and Jessell, T. M. (1995). Floor plate and motor neuron induction by different concentrations of the amino-terminal cleavage product of *sonic hedgehog* autoproteolysis. *Cell* **81**, 445-455.
- Roy, S., Qiao, T., Wolff, C. and Ingham, P. W. (2001). Hedgehog signaling pathway is essential for pancreas specification in the zebrafish embryo. *Curr. Biol.* **11**, 1358-1363.
- Sahly, I., Andermann, P. and Petit, C. (1999). The zebrafish *eyal* gene and its expression pattern during embryogenesis. *Dev. Genes Evol.* **209**, 399-410.
- Sampath, K., Rubinstein, A. L., Cheng, A. M., Liang, J. O., Fekany, K., Solnica-Krezel, L., Korzh, V., Halpern, M. E. and Wright, C. V. (1998). Induction of the zebrafish ventral brain and floorplate requires cyclops/nodal signalling. *Nature* **395**, 185-189.
- Schauerte, H. E., van Eeden, F. J. M., Fricke, C., Odenthal, J., Strähle, U. and Haffter, P. (1998). Sonic hedgehog is not required for the induction of medial floor plate cells in the zebrafish. *Development* **125**, 2983-2993.
- Schier, A. F., Neuhauss, S. C. F., Helde, K. A., Talbot, W. S. and Driever, W. (1997). The one-eyed pinhead gene functions in mesoderm and endoderm formation in zebrafish and interacts with *no tail*. *Development* **124**, 327-342.
- Schulte-Merker, S., van Eeden, F. J. M., Halpern, M. E., Kimmel, C. B. and Nüsslein-Volhard, C. (1994). *no tail* (*ntl*) is the zebrafish homologue of the mouse *T* (*Brachyury*) gene. *Development* **120**, 1009-1015.
- Struhl, G., Barbash, D. A. and Lawrence, P. A. (1997a). Hedgehog acts by distinct gradient and signal relay mechanisms to organise cell type and cell polarity in the *Drosophila* abdomen. *Development* **124**, 2155-2165.
- Struhl, G., Barbash, D. A. and Lawrence, P. A. (1997b). Hedgehog organises the pattern and polarity of epidermal cells in the *Drosophila* abdomen. *Development* **124**, 2143-2154.
- te Welscher, P., Fernandez-Teran, M., Ros, M. A. and Zeller, R. (2002). Mutual genetic antagonism involving GLI3 and dHAND prepatterns the vertebrate limb bud prior to SHH signaling. *Genes Dev.* **16**, 421-426.
- Thisse, C., Thisse, B. and Postlethwait, J. H. (1995). Expression of *snail2*, a second member of the zebrafish *snail* family, in cephalic mesendoderm and presumptive neural crest of wild-type and *spadetail* mutant embryos. *Dev. Biol.* **172**, 86-99.
- Varga, Z. M., Amores, A., Lewis, K. A., Yan, Y.-L., Postlethwait, J. H., Eisen, J. S. and Westerfield, M. (2001). Zebrafish *smoothed* functions in ventral neural tube specification and axon tract formation. *Development* **128**, 3497-3509.
- Waldman, E., Lim, D. and Collazo, A. (2001). Ablation studies on the developing inner ear reveal a propensity for mirror duplications. *Assoc. Res. Otolaryngol. Abs.* **24**, 76.
- Westerfield, M. (1995). *The Zebrafish Book: A Guide for the Laboratory Use of Zebrafish* (*Danio rerio*). Oregon: University of Oregon Press.
- Whitfield, T. T., Riley, B. B., Chiang, M.-Y. and Phillips, B. (2002). Development of the zebrafish inner ear. *Dev. Dyn.* **223**, 427-458.
- Yang, Y., Drossopoulou, G., Chuang, P. T., Duprez, D., Marti, E., Bumcrot, D., Vargesson, N., Clarke, J., Niswander, L., McMahon, A. and Tickle, C. (1997). Relationship between dose, distance and time in Sonic Hedgehog-mediated regulation of anteroposterior polarity in the chick limb. *Development* **124**, 4393-4404.
- Yelon, D., Ticho, B., Halpern, M. E., Ruvinsky, I., Ho, R. K., Silver, L. M. and Stainier, D. Y. R. (2000). The bHLH transcription factor *Hand2* plays parallel roles in zebrafish heart and pectoral fin development. *Development* **127**, 2573-2582.
- Zardoya, R., Abouheif, E. and Meyer, A. (1996a). Evolution and orthology of *hedgehog* genes. *Trends Genet.* **12**, 496-497.
- Zardoya, R., Abouheif, E. and Meyer, A. (1996b). Evolutionary analyses of *hedgehog* and *Hoxd-10* genes in fish species closely related to the zebrafish. *Proc. Natl. Acad. Sci. USA* **93**, 13036-13041.
- Zeng, X., Goetz, J. A., Suber, L. M., Scott, W. J. J., Schreiner, C. M. and Robbins, D. J. (2001). A freely diffusible form of Sonic hedgehog mediates long-range signalling. *Nature* **411**, 716-720.